Molecular Mechanisms of Excitotoxicity:
A Mechanism for Deafferentation-Induced Death and a
Mechanism Underlying the Neuroprotective Effects of Progesterone

A DISSERTATION
SUBMITTED TO THE FACULTY OF THE GRADUATE SCHOOL
OF THE UNIVERSITY OF MINNESOTA
BY

Jessie Irene Luoma

IN PARTIAL FULFILLMENT OF THE REQUIREMENTS
FOR THE DEGREE OF
DOCTOR OF PHILOSOPHY

Paul Gary Mermelstein, Ph.D.

November 2010

To the research animals that make scientific advancement possible.

Abstract

Excitotoxicity leads to neuron death through a variety of mechanisms. Here, the focus is on calcium-mediated mechanisms of apoptosis that are triggered by excessive release of glutamate. Deafferentation of auditory neurons during a developmental critical period induces excitotoxicity within a subpopulation of cochlear nucleus neurons. In the first half of this dissertation, a specific mechanism for deafferentation-induced excitotoxicity of auditory neurons is described. Specifically, FAS death receptor mediated apoptosis is triggered by NFAT-dependent expression of the death receptor ligand FASL. The latter half of this dissertation includes a discussion of the neuroprotective effects of progesterone with regard to excitotoxicity triggered by brain injury. Calcium overload induced by an increase in extracellular glutamate is thought to be a major cause of injury-induced neuron death. There is overwhelming evidence that demonstrates the neuroprotective effects of progesterone against excitotoxicity *in vitro* and in models of traumatic brain injury or stroke injury. Although the use of progesterone as a means of therapy following traumatic brain injury has reached phase III clinical trials, the mechanism by which progesterone exerts its neuroprotective effects remains unknown. I sought to determine the mechanism underlying the neuroprotective effects of progesterone by analyzing the effect of progesterone on calcium signaling. I found that progesterone profoundly inhibits calcium influx through L-type calcium channels and as a consequence, progesterone blocks downstream effectors of calcium signaling.

Interestingly, calcium flux through ionotropic glutamate receptors was unaffected by progesterone. These results suggest a progesterone-sensitive model of excitotoxicity-induced neuron death. In this mechanism, the trigger for excitotoxicity-induced apoptosis occurs by an initial activation of ionotropic glutamate receptors (progesterone insensitive), which leads to neuronal depolarization and secondary activation of L-type calcium channels (progesterone sensitive). The calcium flux through L-type calcium channels activates death-signaling cascades such as the mechanism characterized in the first half of the dissertation where NFAT activation leads to neuronal apoptosis.

Table of Contents

Page

List of Tables

List of Figures

Chapter One

Introduction

Part I: Excitotoxic Death of Neurons

Excitotoxic death of neurons is a complex process that has been shown to occur through a variety of mechanisms that are not yet fully understood. Glutamate-induced excitotoxicty is widely accepted as being a key event in the initiation of neuron death following many types of neuronal insult (Globus et al., 1995; Arundine and Tymianski, 2004; Atif et al., 2009). It is thought that release of this neurotransmitter into the extracellular space occurs sometime shortly after insult, leading to the activation of both ionotropic and metabotropic glutamate receptor mediated signaling pathways.

Excitotoxic Neuronal Death: A Calcium Mediated Process

The activation of ionotropic glutamate receptors ((N-methyl-D-aspartate receptors (NMDARs) and α-amino-3-hydroxy-5-methyl-4-isoxazolpropionic acid receptors (AMPARs)) directly leads to an increase in sodium, potassium, and calcium ion flux, which are key steps in the initiation of neuronal death (Bender et al., 2009; Xu et al., 2009; Schauwecker, 2010). Although many *in vitro* experiments have shown that excitotoxic neuron death depends on the activation of NMDARs and AMPARs, the secondary effects of their activation are critical events in the execution of excitotoxicity. These secondary effects occur by activation of calcium and/or sodium ion influx through either AMPARs or NMDARs leading to depolarization and consequent activation of voltage-gated ion channels such as the L-type calcium channel. In fact, activation of L-type calcium channels appears to play an essential

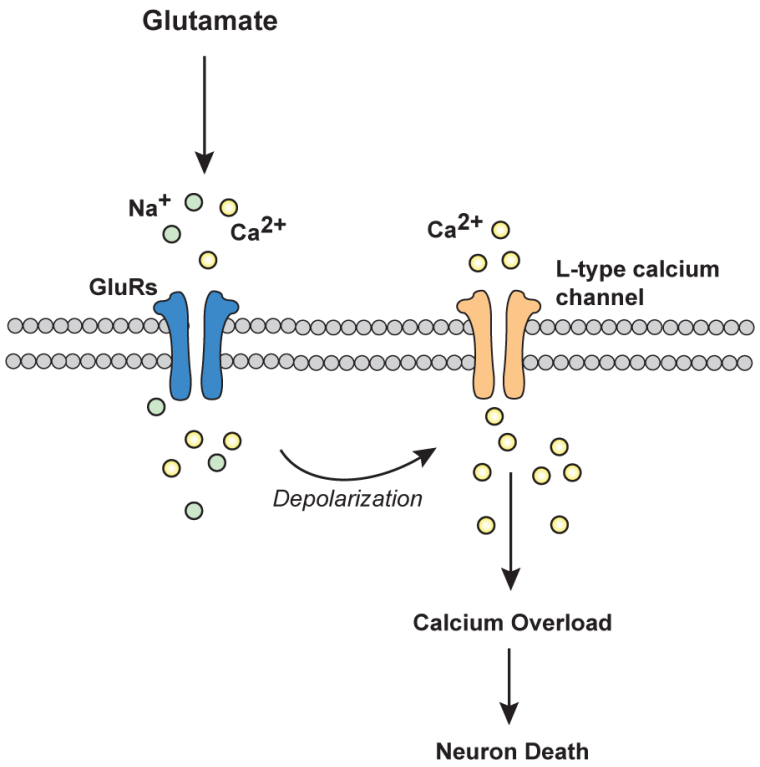

Figure 1. A putative pathway for excitotoxicity. Prolonged stimulation of ionotropic glutamate receptors leads to an influx of sodium and calcium ions that results in neuron depolarization. Consequently, voltage-gated L-type calcium channels are activated to allow calcium influx and subsequent initiation of death pathways.

role in glutamate-induced cell death (Miyazaki et al., 1999; Vallazza-Deschamps et al., 2005; Sribnick et al., 2009). This is consistent with the traditional hypothesis that excitotoxic neuron death results from calcium overload in neurons (Choi, 1985; Tymianski and Tator, 1996; Szydlowska and Tymianski, 2010). A putative pathway

for excitotoxicity that summarizes a way in which glutamate-initiated calcium overload is depicted in Figure 1.

The resulting increase in intracellular calcium can trigger neuron death through intrinsic and extrinsic apoptotic pathways, both of which have been found to occur in excitotoxic cell death. In general, apoptosis is described as the breakdown of cellular components by cysteine proteases known as caspases. There are several caspase isoforms, all of which are activated by proteolytic cleavage. The route through which caspase activation occurs defines whether the apoptotic process is intrinsic or extrinsic. The intrinsic pathway involves activation of caspase-9 through calcium-dependent release of cytochrome c from the mitochondria.

In extrinsic apoptosis, death receptors at the plasma membrane are activated to initiate cleavage of caspase-8 and/or -10. The death receptors belong to the tumor necrosis factor family of receptors (TNFRs), which includes FAS; alternatively known as APO-1, CD95, or TNFR super family 6 (TNFRSF6). The membrane-associated ligand FASL is the endogenous ligand for FAS. One mechanism by which calcium is able to regulate the extrinsic pathway is through its ability to activate the transcription of *fasl*. In this process, calcium binds to and activates calmodulin (CaM) leading to subsequent activation of the phosphatase calcineurin (CN), also known as protein phosphatase 3 (PPP3CA) or protein phosphatase 2B (PP2P). CN dephosphorylates and activates the transcription factor nuclear factor of activated T-cells (NFAT), which binds to the promoter region of *fasl* to activate its transcription (Furuke et al., 1999; Jayanthi et al., 2005). FASL then inserts into the membrane

where it can bind to and activate its receptor FAS to trigger apoptosis. A summary of this pathway is illustrated in Figure 2.

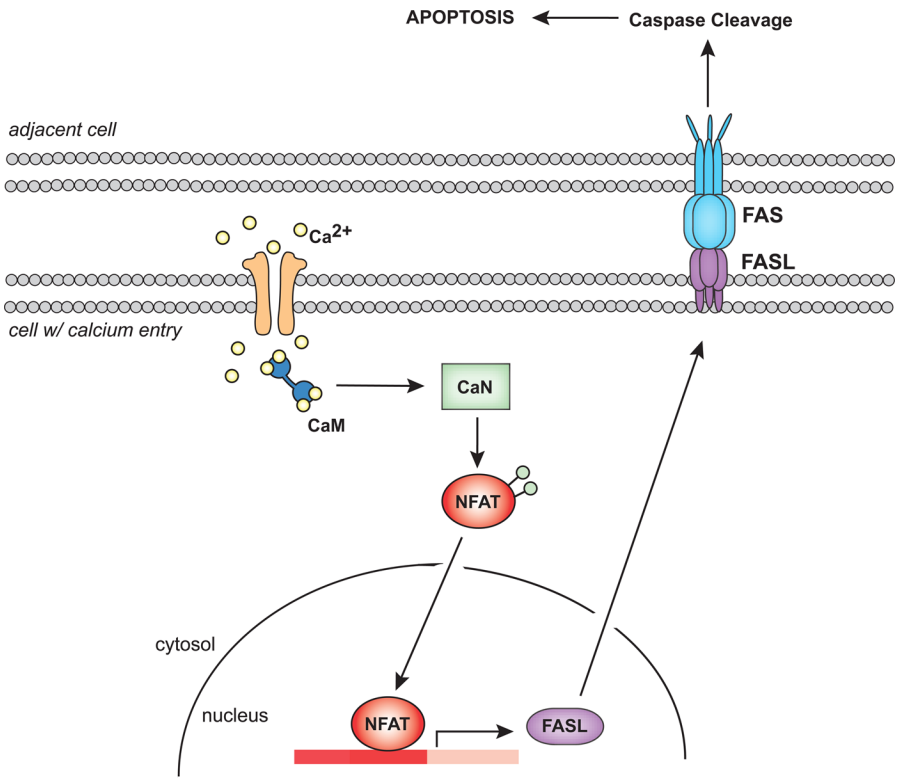

Figure 2. Classical pathway for extrinsic apoptosis mediated by NFAT. Calcium (Ca^{2+}) binds to and activates calmodulin (CaM), which then activates the phosphatase calcineurin (CaN). CaN dephosphorylates NFAT, causing its translocation to the nucleus where it activates the transcription and translation of the death receptor ligand FASL. FASL then inserts into the membrane where it can interact with its receptor FAS on adjacent cells to trigger apoptosis.

Activation of L-type calcium channels leads to the activation of activity-dependent transcription factors like cAMP response element binding protein (CREB) and NFAT (Deisseroth et al., 2003; Weick et al., 2005). Although CREB is often thought of as a survival promoting transcription factor, activation of CREB and/or pathways that lead to CREB activation have also been linked to increased levels of apoptosis (Jimenez et al., 1997; Saeki et al., 1999; Barlow et al., 2006). Interestingly, in certain cell-types, activation of FASL-dependent apoptosis requires the collective efforts of NFAT and CREB. Data collected by others shows that activated NFAT requires the presence of activator protein 1 (AP-1) to induce FASL expression (Macian et al., 2000; Macian et al., 2001). AP-1 is a dimeric transcription factor made up of the immediate early genes Fos and Jun. The activation of CREB is linked to the expression of AP-1, suggesting that it may work in concert with activated NFAT to induce FASL-dependent apoptosis (Sheng et al., 1990). Figure 3 is a canonical pathway by which CREB may act in concert with NFAT to induce FASL expression and consequent apoptosis.

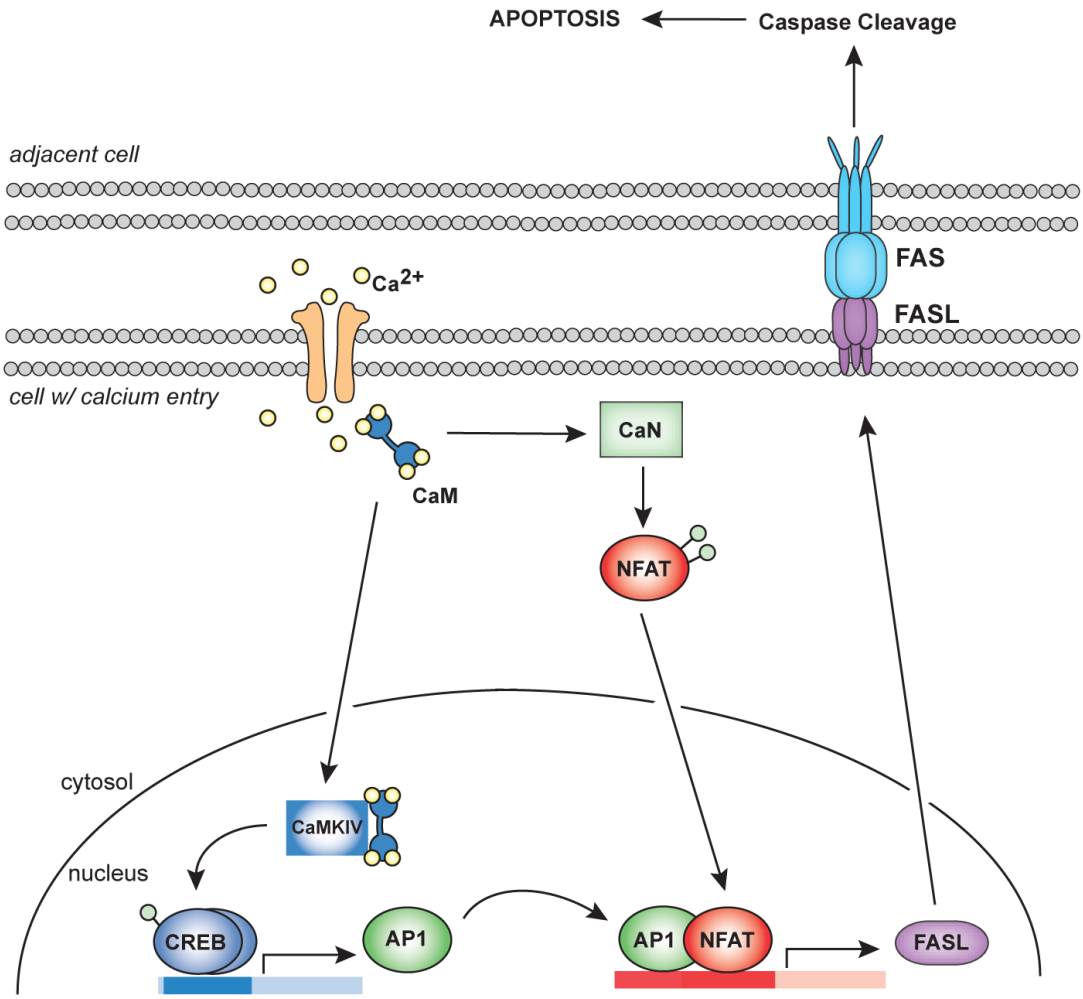

Figure 3. A role for CREB in the initiation of apoptosis. Calcium (Ca^{2+}) binds to and activates calmodulin (CaM), which then activates NFAT as described in Figure 2. Additionally, CaM may also activate CaM-dependent protein kinase IV (CaMKIV), the predominant activator of CREB. CaMKIV then activates CREB, leading to the transcription and translation of activator protein 1 (AP1). AP1 binds with activated NFAT on the promoter of *fasl* to initiate its transcription. Following translation, FASL activates extrinsic apoptosis as formerly described in Figure 2.

Excitotoxic Death of Deafferented Sensory Neurons

Activity-dependent-survival of neurons during a critical period of development is a common theme shared by sensory neurons in the central nervous system (Simmons et al., 1981; Trune, 1982; Born and Rubel, 1985; Lipton, 1986; Hashisaki and Rubel, 1989; Catsicas et al., 1992; Mostafapour et al., 2000). A critical period during development renders primary sensory neurons sensitive to the removal of afferent input wherein a subset of primary sensory neurons die following activity-deprivation. Deafferentation of sensory neurons is thought to lead to degeneration of the innervating axon terminals and subsequent release of glutamate onto the primary sensory neurons causing excitotoxicity-induced neuron death (Parks, 1999; Oertel and Young, 2004; Lu et al., 2007).

In the auditory system, injury or disease can lead to a loss in function of the cochlear hair cells. The primary auditory neurons then become activity-deprived and subsequently die during a developmental critical period. Deafferentation of primary auditory neurons leads to an increase in intracellular calcium that depends upon AMPAR activation (Zirpel et al., 1995a; Zirpel et al., 1998). Solum et al. (1997) found that antagonism of AMPARs during the deafferentation of primary auditory neurons is neuroprotective, which indicates that AMPAR activation contributes to deafferentation-induced neuron death (Solum et al., 1997). While calcium has been

implicated in the death of these auditory neurons, much of the downstream mechanism remains elusive.

It is important that the mechanism of deafferentation-induced neuron death be characterized in order to develop methods of neuroprotection to preserve the functionality of these sensory neurons. During human development, the auditory neurons are sensitive to a loss in afferent input and respond by permanently losing their functionality. The ability to rescue these neurons in children who experience sensorineural hearing loss during development would increase the effectiveness of cochlear implant devices in restoring normal hearing and language skills.

Excitotoxic Death of Injured Neurons and Neuroprotection by Progesterone

Similar to the excitoxic events hypothesized to occur in deafferented sensory neurons, it is thought that both traumatic brain injury and stroke lead to glutamate release from nerve terminals into the extracellular space allowing for prolonged activation of glutamate receptors and initiation of death signaling cascades. While the details of the mechanism for injury-induced death have not yet been defined, methods for protecting neurons against injury-induced death have been recognized. Notably, the neuroprotective effects of progesterone have been well demonstrated such that the therapeutic use of progesterone following traumatic brain injury is now in phase III clinical trials (Goss et al., 2003; Robertson et al., 2006; Sayeed et al., 2006; Wright et

al., 2007; Xiao et al., 2008; Atif et al., 2009). The mechanism that underlies the neuroprotective effects of progesterone remains undetermined.

Traditionally, progesterone is thought to affect variety of reproductive processes and behaviors through a classical genomic signaling pathway. In this pathway, progesterone binds to its classical intracellular steroid hormone receptor, the progesterone receptor (PR). Upon progesterone binding, PR translocates to the nucleus and binds to progesterone response elements (PREs) in the promoter region of target genes to activate their transcription. Progesterone is able to activate this classical signaling mechanism at concentrations in the pico- and nano-molar range. Interestingly, these concentrations of progesterone are not sufficient for neuroprotection, as it must be used at micromolar range concentrations in order to have neuroprotective effects (Goss et al., 2003; Robertson et al., 2006; Sayeed et al., 2006; Wright et al., 2007; Xiao et al., 2008; Atif et al., 2009). Since therapeutically relevant concentrations exceed those necessary for induction of classical signaling, it is possible that neuroprotection by progesterone may occur through a non-receptor mediated mechanism.

Further, data suggesting that the secondary effects of glutamate receptor activation are a critical part of injury-induced death may provide clues as to how progesterone is exerting its neuroprotective effects. For instance, calcium has been shown to be required for excitotoxic neuron death and use of either glutamate receptor or L-type calcium channel blockers have neuroprotective effects following brain injury (Choi, 1985; Tymianski and Tator, 1996; Bender et al., 2009; Xu et al.,

2009; Schauwecker, 2010). This is consistent with the idea that calcium overload occurs by a two-step process: 1) activation of glutamate receptors leads to neuron depolarization and 2) the subsequent activation of voltage-gated L-type calcium channels. Determining whether progesterone affects neuronal calcium signaling via glutamate receptors and/or voltage-gate calcium channels is an important first step in gaining an understanding of the mechanism of neuroprotection by progesterone.

Part II: Summary & Rationale

This dissertation is a discussion of two mechanisms of excitotoxicity that differ by both neuron type and neuronal insult. In the first example of deafferented auditory neurons, the discovery of a neuroprotective strategy was the consequence of characterizing a mechanism for deafferentation-induced neuron death. Therefore, a majority of the discussion regarding deafferented auditory neurons will focus on the steps taken to reveal a mechanism for deafferentation-induced neuron death. In the second example, the unveiling of an excitotoxic mechanism in striatal neurons was corollary to investigating the mechanisms by which progesterone exerts its neuroprotective effects.

A calcium mediated death pathway in deafferented sensory neurons seems likely based upon previous data in the auditory system that 1) demonstrates an increase in intracellular calcium following cochlear removal and 2) shows the necessity of calcium entry through AMPARs for the induction of death of deafferented auditory neurons. Given that the transcription factor NFAT is activated by a calcium-mediated mechanism and that its actions have been implicated in neuronal death pathways, the role for NFAT-dependent death of deafferented auditory neurons is further explored in Chapter 2. Additionally, the characterization of a pathway for deafferentation-induced apoptosis is revealed along with possible methods for neuronal rescue that are based on this pathway.

A well accepted hypothesis states that injury induces excitotoxicity due to excessive accumulation of calcium within neurons. Since progesterone is neuroprotective, it is reasonable to consider that progesterone may modulate calcium signaling in neurons to exert its neuroprotective effects. As such, Chapter 3 includes an analysis of the effects of progesterone on calcium signaling and on the activation of activity-dependent transcription factors NFAT and CREB.

Chapter Two

Deafferentation-Induced Activation of NFAT (Nuclear Factor of Activated T-Cells) in Cochlear Nucleus Neurons During a Developmental Critical Period: A Role for NFATc4-Dependent Apoptosis in the CNS

Introduction

There exists a window of time during development, often referred to as a critical period, when neurons depend on afferent activity for normal growth and survival. This is a common theme shared by all sensory neurons of the CNS (Simmons et al., 1981; Trune, 1982; Born and Rubel, 1985; Lipton, 1986; Hashisaki and Rubel, 1989; Catsicas et al., 1992; Mostafapour et al., 2000). In the auditory system, cochlea ablation (deafferentation) eliminates the primary source of excitatory afferent input to the ipsilateral cochlear nucleus and therefore provides a useful model for studying the effects of deafferentation on the survival or death of cochlear nucleus neurons (Parks, 1999; Oertel and Young, 2004; Lu et al., 2007). In the auditory system, there exists a developmental critical period during which removal of afferent activity results in the death of a significant subpopulation of primary auditory neurons. This phenomenon occurs in the auditory system of several animal models including the anteroventral cochlear nucleus (AVCN) of the mouse and gerbil (Tierney and Moore, 1997; Mostafapour et al., 2000) as well as nucleus magnocellularis (NM) of the chick (Born and Rubel, 1985), the avian homolog of the mammalian AVCN. For example, 61% of AVCN neurons die in mice deafferented at P5; this percentage declines with age and is absent by P14. During maturation, the neurons undergo a transformation from being susceptible to deafferentation-induced death to being resistant to the same manipulation. The biological switch that transforms the way in which these neurons respond to removal of afferent input is yet to be characterized, though many likely cellular and molecular candidates have been

suggested in both the auditory (Rubel, 2004; Harris et al., 2005) and visual (Taha and Stryker, 2005) systems.

Following deafferentation of chick NM neurons, a rapid rise in intracellular calcium concentration (Zirpel et al., 1995a; Barlow et al., 2006). All of the NM neurons show an increase in intracellular calcium concentration but only a subpopulation activate CREB. The pathway culminating in NM neuron death has not been characterized, but has been shown to be calcium-dependent (Zirpel et al., 1998). Neurons in the AVCN of mice also show an increase in intracellular caclium following deafferentation, both during and after the critical period of activity-dependent survival (Zirpel, unpublished). It is therefore plausible to hypothesize that this increase in intracellular calcium causes a cascade of calcium-mediated intracellular signaling events which elicit death response in AVCN neurons within the critical period, but not beyond. Therefore, a cellular mechanism must exist that differentiates the response to increased calcium during the critical period and that is functionally offset by a different intracellular environment due to development (e.g. different gene products and proteins as suggested by Harris and Rubel) or no longer exists following the critical period (Harris et al., 2005).

Calcium/calmodulin activation of the phosphatase calcineurin (CaN; protein phosphatase 2B) results in dephosphorylation of target proteins (Klee et al., 1979; Gupta et al., 1985). One such target is nuclear factor of activated T-cells (NFAT), specifically isoforms c1-c4 (Northrop et al., 1994; Ho et al., 1995; Ruff and Leach, 1995; Molkentin et al., 1998). Dephosphorylation of NFAT leads to exposure of a

nuclear localization sequence, translocation from the cytoplasm to the nucleus (Jain et al., 1993; Rao et al., 1997), and transcription of specific target genes (Ruff and Leach, 1995; Luo et al., 1996; Graef et al., 1999).

Expression of the membrane-bound death receptor ligand, FASL, is mediated by NFAT (Latinis et al., 1997; Holtz-Heppelmann et al., 1998). When FASL binds to its receptor FAS, the intracellular machinery associated with the death receptor FAS is activated and eventually leads to apoptosis by caspase activation and subsequent DNA cleavage (Itoh et al., 1991; Jayanthi et al., 2005). Through this pathway, NFAT-dependent gene expression can actively regulate the induction of extrinsic apoptosis (Kondo et al., 2003; Jayanthi et al., 2005).

The goals of this study were to determine whether or not NFAT plays a role in deafferentation-induced death of cochlear nucleus neurons during the developmental critical period, and to describe a possible pathway through which NFAT mediates neuron death following deafferentation. We show that NFAT activation and FASL expression are increased in the cochlear nucleus following deafferentation during the critical period. Inhibition of NFAT significantly attenuates the increase of FASL expression and neuronal death following deafferentation. These results introduce a novel pathway through which deafferentation-induced death of sensory neurons might be mediated, providing us with a potential strategy for rescuing deafferented sensory neurons from death.

Materials and Methods

Animals and surgery

Postnatal-day 7 (P7), 14, and 21 C57Blk6 mice (Harlan, Indianapolis, IN) were used for these studies, and procedures were approved by the Institutional Animal Care and Use Committee of the University of Minnesota. For all experiments, mice at these three ages were unilaterally deafferented by cochlea ablation (Mostafapour et al., 2000; Zirpel et al., 2000b) while anesthetized with Isoflurane. Ages stated for data are the age at which the surgery was performed. Cochlea ablation was performed by opening the tympanic membrane and removing the middle ear bones with fine forceps. The cochlear chamber was then penetrated with fine forceps and the cochlear epithelium and modiolus were completely aspirated from the chamber through a pulled glass pipette with an approximate tip diameter of 0.7 mm. For P7 mice, a small incision was made inferior to the pinna in order to expose the ear canal. This incision was closed with cyanoacrylate glue following surgery. Mice were then returned to their cages with their mother until sacrificed. After sacrifice, a thick coronal section containing the brainstem was made with a razor blade and immediately immersed in oxygenated artificial cerebral spinal fluid while cochlear nuclei or whole brainstems were dissected and collected. Complete removal of the cochlea and modiolus was verified by examination of the cochlear bulla. For collections of cochlear nuclei, the nuclei on the side of the brain ipsilateral to deafferentation were collected as deafferented tissue and the nuclei on the side of the

brain contralateral to deafferentation were collected as control, or non-deafferented tissue. Tissue margins were determined using figures 73-78 in The Mouse Brain Atlas (Paxinos and Franklin, 2001) as a guide to track the AVCN as well as the superficial glial zone and granular layer of the cochlear nucleus that mark the termination of the AVCN and the start of the posterior cochlear nucleus and the dorsal cochlear nucleus.

Drugs and administration

11-R VIVIT (Calbiochem, Darmstadt, Germany), a cell-permeable peptide NFAT inhibitor, was dissolved in sterile saline to 8.40 mM and injected at concentrations of either 20 mg/kg or 30 mg/kg. A higher dose of 35 mg/kg was injected but resulted in death of the animals shortly after injection. FK506 (Sigma-Aldrich, Saint Louis, MO), a CaN inhibitor, was dissolved in DMSO to 3 mg/mL and then further diluted in sterile saline to 1.0 ng/ul and injected at a dose of 1 mg/kg. Injections were made with a 10 µl microsyringe and 30 ½ gauge needle. Mice were anesthetized and the area posterior to the bulla on the right side of the head was sterilized with 70% ethanol before receiving injection into the cerebral spinal fluid (CSF). The area posterior to the bulla and just beneath the skull is in close contact with the right cochlear nucleus, allowing for efficient drug delivery to the cochlear nucleus neurons. This was verified by injection of Fast Green dye and visual verification of dye diffusion to the CSF surrounding the cochlear nucleus and staining

of the cochlear nucleus neurons with the Fast Green dye. Saline injections of 2 µl were administered for vehicle control (2 µl was the maximum volume injected into a drug treated animal). Drug injections were performed 90 minutes prior to surgery.

Fractionation of cellular lysates

Cytoplasmic and nuclear extracts were prepared using a nuclear and cytoplasmic extraction kit, NE-PER (Pierce, Rockford, IL). The protocol provided with the kit was followed with minor revisions. Cochlear nuclei were collected into 300 µl of cytoplasmic extraction reagent (CER) I containing 1X protease inhibitor cocktail (Pierce) and 1X phosphatase inhibitor cocktail (Pierce). Samples were immediately homogenized with 7 strokes (4×pestle A; 3×pestle B) in a 1 ml Dounce homogenizer, vortexed at highest setting for 15 seconds, and incubated on ice for 10 minutes. Then, 16.5 µl ice-cold CER-II was added to each sample, vortexed for 5 seconds, and centrifuged at 14,000 × g for 5 minutes. The supernatant was collected as the cytoplasmic fraction. The nuclear pellet was suspended in 100 µl nuclear extraction reagent (NER) containing 1X protease inhibitor (Pierce) and vortexed on high for 15 seconds every 10 minutes for 40 minutes. This was followed by centrifugation at 14,000 × g for 10 minutes and collection of the supernatant as nuclear lysate. All samples were kept on ice throughout the procedure. Centrifugation was performed at 4ºC. Concentrations were determined using the BCA

Protein Assay Kit (Pierce). Lysates were stored at -80ºC until used for Western blotting.

Western blot

Cochlear nuclei were collected into ice cold RIPA buffer containing 50 mM Trizma, 1 mM EDTA, 1% Triton X-100 with 1X protease inhibitor cocktail (Pierce) and 1X phosphatase inhibitor cocktail (Pierce) and immediately homogenized with tissue tearor while on ice. Samples were then centrifuged at 14,000 × g for 15 minutes at 4ºC. Supernatant was collected and BCA assay was used to determine protein concentration. For a total sample volume of 37 µl, lysates containing 30 µg of protein were diluted with β-mercaptoethanol (1:100), 4X LDS (lithium dodecyl sulfate) buffer (final concentration 1X), and dH_2O, heated to 95ºC for 10 minutes, and centrifuged for 5 minutes at 14,000 × g. Samples were separated into a 10% SDS polyacrylamide gel and blotted onto a nitrocellulose membrane. Membranes were then cut in half in order to assay the high molecular weight bands separately from the low molecular weight bands. Membranes were washed with 0.1 M phosphate buffered saline (PBS; pH 7.4) with 5% (w/v) powdered milk for 1 hour, then incubated (overnight 4ºC) with one of the following primary antibodies diluted in PBS with 0.1% Triton X-100 (PBST) and 5% (w/v) powdered milk (antibody buffer): rabbit polyclonal anti-NFATc4 (1:200; Santa Cruz Biotechnology Inc., Santa Cruz, CA), mouse monoclonal GAPDH (1:20000; Chemicon, Temecula, CA), or rabbit

polyclonal anti-CREB (1:1000; Upstate). Membranes were washed in PBST 5×5 minutes and incubated with one of the following secondary antibodies diluted in antibody buffer: goat anti-mouse Alexa-680 (1:20000; Invitrogen Corp., Carlsbad, CA) or goat anti-rabbit IRDye 800 (1:20000; LI-COR Biosciences, Lincoln, NE). Membranes were washed 7×5 minutes and scanned with a LI-COR Odyssey infrared imaging system. The integrated intensity of fluorescence for each band (NFATc4, ~120 kDa; FASL, 45 kDa; GAPDH, 38 kDa) was then determined. All levels were normalized to GAPDH levels. For fractionation analysis, the amount of nuclear translocation of NFATc4 was determined by first calculating the amount of nuclear NFATc4 in each sample set (Control or deafferented): $NFATc4_{nucleus}$: $NFATc4_{total}$. These values were then used to calculate the percent increase of nuclear NFATc4 following deafferentation: ((nuclear $NFATc4_{CX}$:nuclear $NFATc4_{CTL}$)-1)×100) (CX=deafferented; CTL=control). CREB is localized to the nucleus in AVCN neurons (Tang, Luoma, and Zirpel; unpublished) and was used to verify complete separation of nuclear lysate from cytoplasmic lysate.

Immunohistochemistry

Following deafferentation for the desired amount of time, brainstems were dissected from the cranium and immediately immersed and fixed in PBS with 4% paraformaldehyde at 4°C overnight, then 30% sucrose overnight at 4°C before embedding in cryogenic OCT medium and freezing. Twenty μm cryosections were

collected on gelatin-subbed slides and dried on a warming plate for 30 minutes. Immunohistochemistry for NFATc4 was carried out by first re-hydrating sections in PBS 10 minutes, incubation in blocking buffer (0.1 M PBS, 1% bovine serum albumin, 2% normal goat serum) 1 hour at room temperature (RT: ~70º F), and incubation with primary antibody (1:100, rabbit polyclonal anti-NFATc4, Santa Cruz Biotech or PBS for negative control) in blocking buffer with 0.3% Triton X-100 (antibody buffer) for 48 hours at RT in a humidity chamber. Sections were then washed in PBS 3×5 minutes and incubated with secondary antibody (1:1000, goat anti-rabbit Alexa-594, Invitrogen) in antibody buffer for 1 hour at RT. Sections were washed 5×5 minutes and mounted with FluorSave™ (Calbiochem). Apoptotic cells were identified using ApopTag Fluorescein *In Situ* Apoptosis Detection Kit (Chemicon). Product protocols were followed exactly. As a positive control, sections were pretreated with DNase buffer (30 mM Trizma, pH 7.2, 4 mM $MgCl_2$, 0.1 mM dithiothreitol (DTT)) for 5 minutes at RT, DNase I (1000U/ml; Invitrogen) for 10 minutes at RT, and 5×3 minute PBS washes before proceeding with the protocol. This resulted in ApopTag labeling of nearly all cells. As a negative control, TdT (terminal deoxynucleotidyl transferase) was replaced with PBS, which resulted in no labeled cells.

Fluorescently labeled cells were visualized with a Nikon TE300 Eclipse microscope using either a 100x or 40x Fluor oil objective, filter cube sets 31004 (Alexa594), 31000v2 (DAPI), and 41017 (ApopTag) from Chroma (Rockingham, VT), and a xenon light source (Sutter Instrument Company, Novato,CA). Digital

images were acquired with a cooled CCD camera (Photometrics CoolSNAP Hq or Cascade 512f, Roper Scientific; Tucson, AZ) and MetaMorph Software (Universal Imaging Corp., West Chester, PA). Images were processed/analyzed using Adobe Photoshop. Neurons in the AVCN were discerned from glia by morphology. For each animal, three images of both the left and right AVCN were taken from each of four separate sections (12 images of each AVCN) and used for cell counting. Values were averaged to obtain a single value for the left (control) and right (deafferented) AVCN per animal. Counts made were of neurons positively labeled for ApopTag, NFATc4 (cytoplasmic and/or nuclear), or only nuclear NFATc4. Nuclear staining was determined by overlap of NFATc4 staining with DAPI nuclear staining. To calculate the relative amount of nuclear NFATc4, the number of neurons positive for nuclear NFATc4 was divided by the total number of neurons positive for NFATc4 (cytoplasmic and/or nuclear). The effect of deafferentation on the level of nuclear NFATc4 was determined by calculating the percent increase of nuclear NFATc4: ((the ratio of nuclear NFATc4 on deafferented side: control side-1)×100). For immunohistochemical analysis, the change in nuclear NFATc4 was also verified by comparing the total area of NFATc4 and DAPI colocalization to the total area per image and was consistent with the reported cell count data.

Cell counts

At least four animals were used for each experimental group. Frozen sections 20 μm thick were collected on microscope slides and stained using the following cresyl violet Nissl staining procedure: 100% EtOH 2 minutes, Xylenes 2 minutes, 100% EtOH 2 minutes, 70% EtOH 2 minutes, 20% EtOH 2 minutes, dH_2O 5 minutes, cresyl Violet solution (0.1% (w/v) cresyl violet, 3% acetic acid) 5 minutes, 2 dips in dH_2O, 2 dips in differentiation solution 1 (70% EtOH, 10% acetic acid), 2 dips in differentiation solution 2 (100% EtOH, 10% acetic acid), 100% EtOH 1 minute, Xylenes 2 minutes, then mounted with Permount (Sigma-Aldrich).

Four sections of each AVCN were chosen for counting, making sure to include anterior, middle, and posterior portions of the AVCN along the rostral/caudal axis. For each section, four 40X images of the AVCN were acquired to include ventral, middle, and dorsal portions along the medial/lateral axis of the nucleus in the cell counts. The total number of neurons in each 40X image was obtained, excluding glial cells based on morphology. Counting was performed by an unbiased observer with no knowledge of the treatment group being counted. The average number of neurons per 40X image was then calculated for each AVCN nucleus analyzed. The averages were used to compare the number of AVCN neurons ipsillateral to deafferentation versus contralateral to deafferentation for each animal. The percent of neuron loss following deafferentation was calculated for each animal using the following equation: (1- (deafferented # of neurons/ intact # of neurons))×100.

Polymerase chain reaction (PCR)

Total RNA was isolated from cochlear nuclei collected in RNAlater reagent using the RNeasy Micro Kit and protocol (Qiagen). Tissue was homogenized with motorized tissue homogenizer followed by centrifugation through Qiashredder membrane (Qiagen). Total RNA was eluted with 13 µl of sterile distilled H_2O and yielded approximately 1 µg of RNA. cDNA was synthesized by adding the following to the total eluted RNA: 1 µl oligo D_{T20} (0.5 µg/ml) and 1 µl dNTP mix (10 mM). Mixture was heated to 65ºC for 5 minutes, put on ice for 1 minute, then (in µl) 4 of 5X first-strand buffer, 1 of DTT (0.1 M), 1 of RNaseOUT (40 U/µl), and 1 of SuperScript III RT (200U/µl) were added to each sample before incubation at 25ºC for 5 minutes, 53ºC for 50 minutes, and 70ºC for 15 minutes. Finally, 1 µl of RNase-H was added to each cDNA sample and incubated at 37ºC for 20 minutes. All RT reagents were purchase from Invitrogen. The cDNA was diluted to 40 ηg/µl with sterile dH_2O and 1 µl per reaction was used. Forward and reverse primers were diluted with sterile dH_2O to 3.0 µM and a mix was made containing both forward and reverse primers at 1.5 µM. Primer sequences used were ACCACAGTCCATGCCATCAC (forward *gapdh*), CCACCACCCTGTTGCTGTA (reverse *gapdh*), AGCTACCTGGGGGCAGTATT (forward *fasl*), GCTTATACAAGCCGAAAAAGG (reverse *fasl*), TGCTGGTACCAATCTCATGG

(forward *fas*), TCTGGGGTTGATTTTCCAAG (reverse *fas*), CCGAAGTGGAGCAGAAGAAG (forward *s15*), CTCCACTGGTTGAAGGTC (reverse *s15*), TCATTGACACCACCTCCAAA (forward *rpl3*), and GCACAAAGTGGTCCTGGAAT (reverse *rpl3*). Each 30 µl PCR reaction contained (in µl) 15 of DyNAmo HS SYBR green master mix (New England Biolabs, Ipswich, MA), 6 of primer mix, 6 of cDNA template, and 3 of dH_2O. The thermocycling protocol was as follows: 95ºC for 15 minutes, 94ºC for 10 seconds, 60ºC for 30 seconds, 72ºC for 30 seconds, and fluorescence data acquisition for a total of 40 cycles. Melting curves were generated to verify the specificity of the generated products. Each reaction was run in triplicate. Controls for DNA contamination of reagents were run using dH_2O in place of cDNA template and all yielded no PCR product as expected. Fluorescence of the SYBR green was detected using the Opticon2 thermocycler (MJ Research, Waltham, MA). Ct (cycle at which threshold fluorescence is reached) values for each sample were then collected at a threshold level of fluorescence set within the linear phase of amplification. All samples were analyzed using the semi-quantitative ΔΔCt method (Livak and Schmittgen, 2001) comparing expression between the deafferented and intact cochlear nuclei. Results are reported as mean-fold changes in expression following deafferentation ($2^{-\Delta\Delta Ct}$). All values were normalized to *gapdh* (or either *s15* or *rpl3* when noted) to control for loading. *gapdh* was used again, as it has not been previously shown to be upregulated or degraded in the early stages of cell death.

Analysis and Statistics

At least three biological replications were performed for each experiment. For Western blots and semi-quantitative RT-PCR, the cochlear nucleus tissue from three mice was pooled for each replicate. Control levels for each treatment group were not significantly different from each other and the data were therefore normalized to their respective control, or non-deafferented values (deafferented:control). When ratios of deafferented:control were calculated, a paired t-test was performed to determine if the means were significantly different from the hypothetical value of 1.0 (indicated on graphs with a dotted line at 1.0), a value indicating no change following deafferentation. Data are reported as the mean ± SEM. ANOVAs with Bonferroni post-hoc tests were used to determine the difference between group means. A single value greater than two standard deviations from the mean was removed from the RT-PCR non-drug treated deafferentation group. All statistical analyses were calculated using Prism 4.0 software (GraphPad Software, Inc., San Diego, CA).

Results

Activation of NFATc4 occurs only within the critical period of dependence on afferent activity for survival

A critical period during development when AVCN neurons are susceptible to deafferentation-induced death previously showed that deafferentation of AVCN neurons resulted in a ten-fold increase of apoptotic neurons at P7 and no increase at P21 as shown with TUNEL assay (Terminal Deoxynucleotidyl Transferase Biotin-dUTP Nick End Labeling) (Mostafapour et al., 2000). These results were reproduced in this study as described by the following experiment. Mice at ages P7, P14, and P21 underwent unilateral deafferentation in order to remove afferent input from cochlear nucleus neurons while leaving the contralateral side intact as a control to which the deafferented tissue could be compared. This control was chosen because no difference in neuron death is observed between the AVCN neurons of mice that have not undergone deafferentation compared to the AVCN neurons contralateral to deafferentation. The cochlear nucleus neurons were deafferented for 24 hours and labeled with ApopTag; a fluorescent TUNEL stain that labels fragmented DNA and indicates induction of apoptosis. The 24 hour time point was chosen because TUNEL labeling of AVCN neurons was previously shown to be maximal following deafferenation at this time (Mostafapour et al., 2000). Intact AVCN neurons contralateral to deafferentation at each age examined showed very few apoptotic neurons. However, in AVCN neurons ipsilateral to deafferentation, apoptotic neurons

at P7 were abundant. When deafferentation was performed at either P14 or P21 there were very few apoptotic neurons in the deafferented AVCN (Figure 1A). Quantification of these data showed that deafferentation at P7 for 24 hours leads to a significant increase in the number of apoptotic AVCN neurons compared to control. This is in contrast to deafferentation at P14 and P21 when deafferentation did not result in an increase of apoptotic AVCN neurons (Table 1 & Figure 1B). In order to confirm that ApopTag-labeled AVCN neurons eventually lead to death and a decrease in neuron number in the AVCN, neuron counts were performed following 96 hour deafferentation, a time at which loss of AVCN neurons following deafferentation has reached a maximum (Mostafapour et al., 2000). In mice deafferented at P7, the percent loss of AVCN neurons was significant whereas at P14 and P21 the loss was absent (Table 1 & Figure 1C). These data demonstrate that there is a developmental critical period during which the AVCN neurons are susceptible to deafferentation-induced apoptosis that leads to neuron loss and that this critical period includes mice at age P7 but not ages P14 or P21, which are outside of this critical period. This is consistent with the results reported by Mostafapour et al. (2000).

Both an increase in intracellular calcium concentration and calcium-dependent CREB-phosphorylation have been shown to result from removal of afferent input to auditory neurons (Zirpel et al., 1995a; Zirpel et al., 2000a). Since the activation of the transcription factor NFATc4 is mediated by calcium (Jain et al., 1993; Crabtree and Olson, 2002), we wanted to determine if NFATc4 was activated in deafferented AVCN. NFATc4 is the predominant NFATc isoform in nervous tissue and is

expressed in mouse brainstem nuclei (Bradley et al., 2005). NFATc4 translocates from the cytoplasm to the nucleus upon dephosphorylation and activation by CaN following a calcium signal that activates CaM (Ruff and Leach, 1995; Woischwill et al., 2005). Therefore, NFAT activation was measured by the change in the amount of nuclear NFATc4 following deafferentation. Quantification was done by Western blot analysis of fractionated cytoplasmic and nuclear lysates from cochlear nucleus tissue. At ages P7, P14, and P21 NFATc4 was localized to the cytoplasm (C) of intact cochlear nucleus tissue.

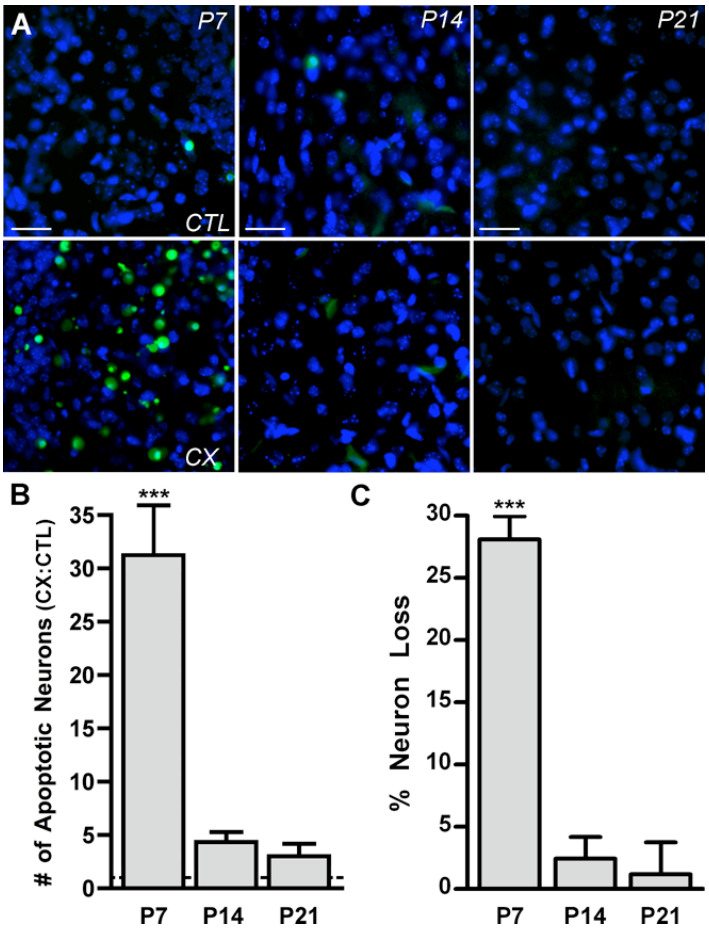

Figure 1. Apoptosis and neuron death result from deafferentation during a developmental critical period. (A) Fluorescent photomicrographs of AVCN tissue labeled with ApopTag (green) and DAPI (blue) at P7, P14, and P21 following 24 hour deafferentation. The intact AVCN (CTL; upper panels), and the deafferented (CX) (lower panels) are shown at each age. ApopTag labeling is prevalent at P7 following CX, but absent at P14 and P21. Scale bar represents 75 μm. (B) Comparison of number of apoptotic AVCN neurons on the CX side vs. the CTL side were made (CX:CTL) to demonstrate the effect of CX on neuron death in the AVCN. Cochlear nucleus neurons of P7 mice, but not P14 or P21 mice, showed significantly more apoptotic neurons on the CX vs. the CTL side 24 hours post-surgery (31.26 ± 4.68; n=6; t=7.90; ***p<0.001). Means were compared to 1.0. (C) Percent loss of AVCN neurons following 96 hour CX as assayed from neuron counts of cresyl violet stained sections. At age P7 there is significant loss of AVCN neurons (28.08 ± 1.31; n=4; t=21.52; *** p<0.001; means compared to 0.0), but no significant loss at P14 or P21.

	Mean # of Neurons per Sampled Area (± SEM)		% Neuron Loss (±SEM)		Mean # of Apoptotic Neurons per Sampled Area (± SEM)	
Age at Surgery (Postnatal day)	CX	Control		n	CX:Control	n
7	36.46 ± 1.86	50.00 ± 1.61	28.08 ± 1.31	4	31.26 ± 4.68	6
7 (+ 20 mg/kg 11R-VIVIT)				n/a	10.80 ± 2.98	7
7 (+ 30 mg/kg 11R-VIVIT)	49.60 ± 2.84	57.82 ± 3.73	11.08 ± 0.91	4	6.45 ± 0.40	5
7 (+ FK506)	51.50 ± 1.32	55.63 ± 1.84	8.00 ± 1.41	4	4.31 ± 0.96	4
14	44.85 ± 2.12	45.00 ± 2.16	2.66 ± 0.85	4	2.43 ± 0.59	4
21	43.09 ± 1.25	43.92 ± 2.26	1.52 ± 1.44	5	3.00 ± 1.17	5

Table 1. Number of AVCN neurons following 96 hour deafferentation (CX) or number of apoptotic AVCN neurons following 24 hour CX.

However, 15 minutes after deafferentation, NFATc4 was detected in the nuclear lysate (N) at P7, but not P14 or P21 (Figure 2A). Western blots (as shown in Figure 2A) with cochlear nucleus tissue that underwent deafferentation for 15, 30, or 45 minutes were analyzed and demonstrated a time-course of NFATc4 nuclear translocation following deafferentation. The amount of NFATc4 in the nuclear lysate increased rapidly (within 15 minutes) at age P7 and returned to control levels by 30 and 45 minutes (Figure 2B). Together, these results demonstrate that cochlear nucleus neurons of P7 mice are within a critical period of susceptibility to deafferentation-induced death, and that deafferentation for as little as 15 minutes results in rapid and transient activation of NFATc4 in AVCN tissue as demonstrated by an increase in nuclear NFATc4.

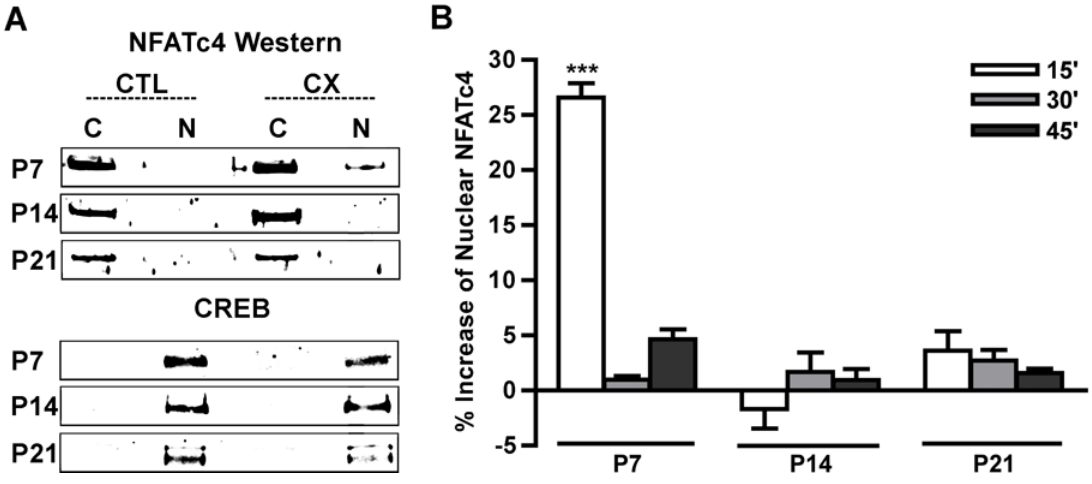

Figure 2. NFATc4 is activated in the cochlear nucleus following deafferentation during a developmental critical period. (A) Data of Western blots with fractionated AVCN cellular lysates. NFATc4 is localized to the nuclear lysate (N) 15 minutes post-deafferentation (CX) at P7, but not P14 or P21 when it is predominantly localized to the cytoplasm (C) in both the CX and the intact (CTL) AVCN. CREB is shown as a control for efficient separation of nuclear and cytoplasmic lysates, as it is localized to the nucleus in AVCN neurons. (B) Quantification of Western blots of cytoplasmic and nuclear lysates. Percent increase of nuclear NFATc4 15 minutes (as shown in A) 30 minutes, and 45 minutes post-CX. Significant increase of nuclear NFATc4 is seen only at P7 15 minutes post-CX (26.6% ± 1.28; n=3; t=16.08; ***p<0.001; means compared to 0.0 with paired t-test).

To confirm that NFATc4 is activated in the neurons of the AVCN (versus glia) the subcellular localization of NFATc4 following deafferentation was analyzed using immunohistochemistry (Figure 3 A-D). AVCN sections were labeled with NFATc4 (red) and DAPI for identification of nuclei (blue). For ages within (P7) and outside of (P14 and P21) the critical period there was very little colocalization of DAPI and NFATc4 in the intact AVCN neurons, indicating that NFATc4 is in an inactive state and resides in the cytoplasm under normal conditions (Figure 3A-D*;* upper). In deafferented AVCN neurons, NFATc4 was significantly increased in the neuronal nuclei 15 minutes following deafferentation at P7 as shown by the colocalization (green) of NFATc4 and DAPI (Figures 3 A,B). Magnification of the boxed area in Figure 3A is shown so that the colocalization can easily be visualized (Figure 3B). At ages outside of the critical period (P14 and P21), the amount of colocalization remained unchanged following deafferentation, indicating that

NFATc4 does not translocate to the nucleus following deafferentation at ages outside of the critical period (Figure 3 C & D). Quantification of the increase in nuclear NFATc4 in AVCN neurons following deafferentation for 15, 30, 45, or 60 minutes showed that the amount of NFATc4 in the nucleus at P7 (□) increased significantly following 15 minute deafferentation. This level decreased with time but remained significant 30 and 45 minutes post-deafferentation. The increase at P7 was absent by 60 minutes post-deafferentation. No increase in nuclear NFAT occurred for any of the time-points at P14 (▲) or P21 (◯) (Figure 3E). These results indicate that deafferentation induces NFATc4 activation in AVCN neurons during the critical period, and that NFATc4 is in an active state for up to 45 minutes post-deafferentation.

NFAT dependent apoptosis

The cell-permeable peptide 11R-VIVIT binds to the calcium-mediated phosphatase CaN and specifically blocks its ability to activate NFAT, leaving other substrates targeted by CaN unaffected (Aramburu et al., 1999; Noguchi et al., 2004). Additionally, FK506 is a less-specific inhibitor of NFAT that works by inhibiting CaN (Liu et al., 1991; Steiner et al., 1992).

To determine if *in vivo* treatment with 11R-VIVIT or FK506 blocks activation of NFATc4 in the AVCN of P7 mice, animals were pretreated with 30 mg/kg of 11R-VIVIT (VIV), 1 mg/kg FK506, or saline as vehicle control (sal). NFATc4 activation was determined by calculating the percent increase of nuclear NFATc4 within the

AVCN on the side ipsilateral to deafferentation compared to the side contralateral to deafferentation by Western blot analysis of fractionated lysates (Figure 4A).

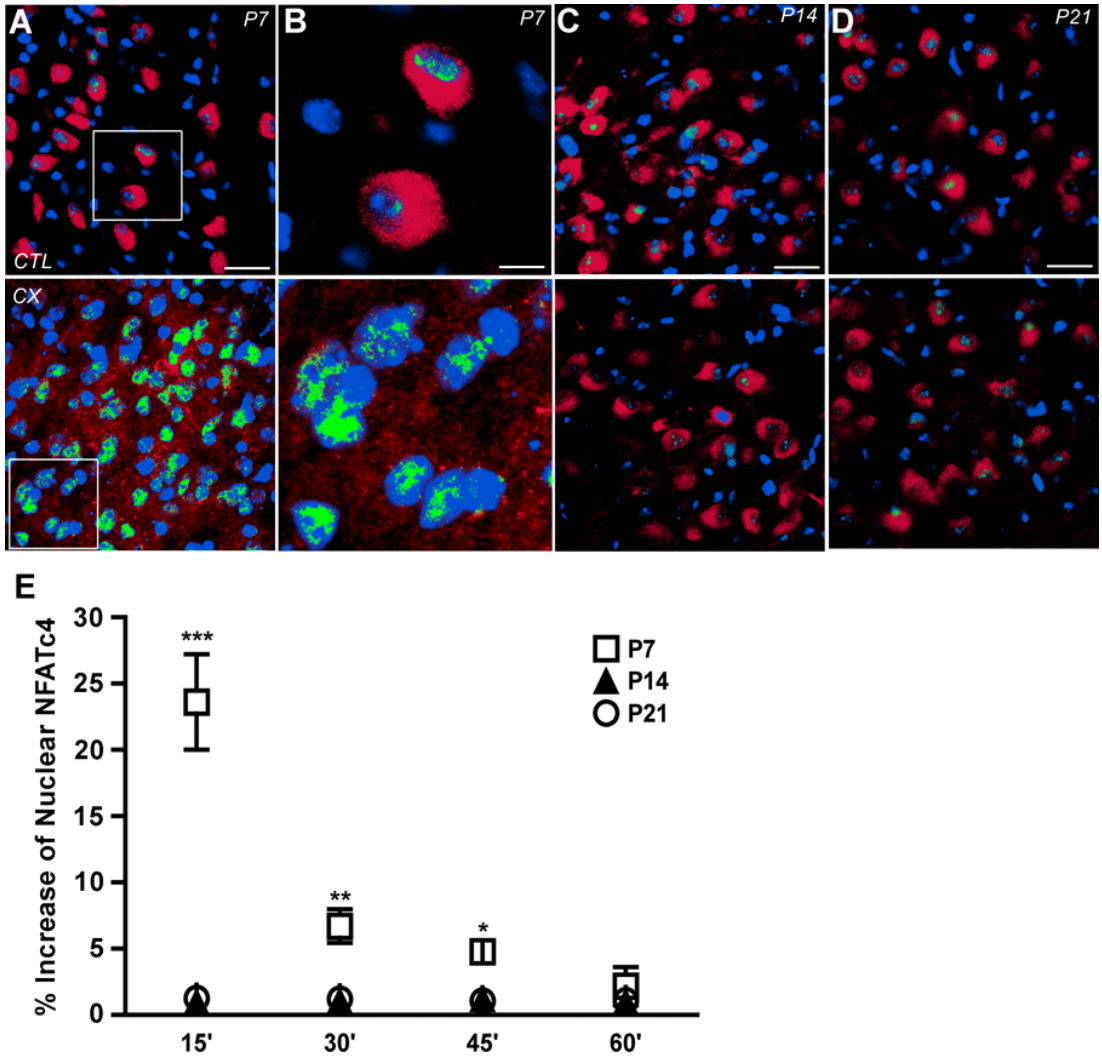

Figure 3. NFATc4 is activated in AVCN neurons following deafferentation during a critical period of development. (A-D) Fluorescent photomicrographs of AVCN. Intact (CTL) and 15 min deafferentation (CX), labeled with NFATc4 (red), DAPI nuclear counterstain (blue), and the colocalization of NFATc4 and DAPI (green). (A) Marked colocalization of NFATc4 and DAPI is shown on the side

ipsilateral to CX at P7. (B) Magnification of the boxed area is shown in A. (C) P14 and (D) P21; Little to no colocalization in either the CTL or CX AVCN neurons following CX. (E) Analysis of immunohistochemical images of mice deafferented for 15, 30, 45, or 60 minutes shows a time-course for nuclear translocation of NFATc4. Nuclear NFATc4 significantly increases in the AVCN neurons at P7 (□) 15 minutes (23.62% ± 4.51; n=3; t=16.14; ***p<0.001), 30 minutes (6.71% ± 4.51; n=3; t=4.58; **p<0.01), and 45 minutes (4.78%% ± 4.50; n=3; t=3.27; *p<0.05) following CX. P14 (▲) and P21 (◯) AVCN show no significant increase of nuclear NFATc4 following CX for any of the time-points. Scale bars represent 75 μm (A,C,D) and 25 μm (B). Data analyzed with two-way ANOVA.

Pretreatment with VIV or FK506 abolished the deafferentation-induced increase of nuclear NFATc4. Pretreatment with sal did not differ from the untreated group, and both groups showed an increase of nuclear NFATc4 post-deafferentation (Figure 4A). These data demonstrate that both VIV and FK506 are effective at inhibiting NFATc4 activation *in vivo*.

Recently, the activation of NFATc4 has been linked to the induction of apoptotic pathways in the central nervous system following drug administration and ischemia (Jayanthi et al., 2005; Zhang et al., 2005). Since we have shown that deafferentation induces NFATc4 activation in AVCN neurons at ages that are susceptible to deafferentation-induced apoptosis, we asked whether or not deafferentation-induced apoptosis is dependent on the activation of NFAT. Images of deafferented P7 AVCN neurons showed plentiful labeling with ApopTag in both untreated and saline treated animals (Figure 4B). In contrast, ApopTag labeling was

significantly reduced in animals pretreated with 30 mg/kg 11R-VIVIT (VIV 30) (Figure 4B). Ratios of the number of ApopTag labeled AVCN neurons on the deafferented side versus the intact side were significantly attenuated in mice pretreated with 20 mg/kg 11R-VIVIT (VIV 20), 30 mg/kg 11R-VIVIT (VIV 30), or FK506 (Table 1 & Figure 4C). Means were also compared to 1.0 with a paired t-test to determine if the deafferentation-induced ApopTag labeling was statistically significant; values are expressed as a ratio of the number of apoptotic neurons in deafferented to control and 1.0 represents no change following deafferentation. The results indicate that treatment with VIV 30, FK506 or VIV 20 did not completely eliminate an increase in the induction of apoptosis following deafferentation. The data in Figure 4 suggest that NFAT plays a role in the deafferentation-induced apoptosis of AVCN neurons in mice at P7, an age within the critical period.

To verify that death results from the initiation of apoptosis in deafferented AVCN neurons, neuron number was analyzed and compared between the deafferented and control AVCN neurons of P7 mice. Following a 96 hour deafferentation, a time when neuron loss in the AVCN reaches a maximum in P7 mice (Mostafapour et al., 2000), images of cresyl violet stained AVCN sections were acquired. The AVCN of P7 mice had more neurons on the side contralateral to deafferentation (Figure 5A) versus ipsilateral to deafferentation (Figure 5B). Mice pretreated with 11R-VIVIT showed less neuron loss between the AVCN contralateral to (Figure 5C) versus ipsilateral to deafferentation (Figure 5D).

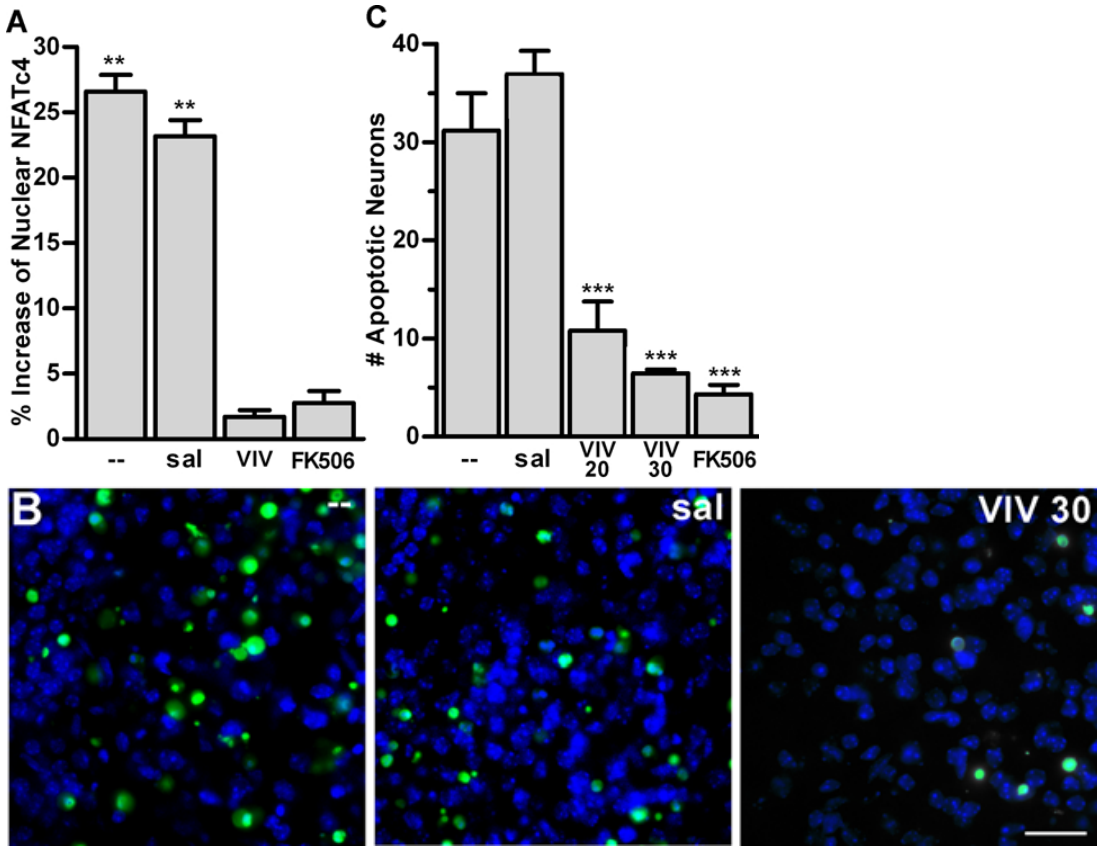

Figure 4. Activation of NFATc4 is a precursor to induction of apoptosis during the developmental critical period. (A) Data of Western blot analysis of cellular fractions. Pretreatment with 30 mg/kg of the NFAT inhibitor peptide 11R-VIVIT (VIV) or CaN inhibitor FK506 attenuated the increase of nuclear NFATc4 in the cochlear nuclei of P7 mice 15 minutes post-deafferentation (CX). Pretreatment with saline (sal) served as a vehicle control (23.19% ± 1.24; t=18.67;**p<0.01) and did not differ from untreated (--) animals (26.60 ± 1.28; t=20.74;**p<0.01). Using paired t-tests, means were compared to 0.0. (B) Fluorescent photomicrographs of ApopTag labeled AVCN neurons of P7 mice 24 hours post-CX. Images shown are AVCN on the side ipsilateral to CX. Pretreatment with 30 mg/kg (VIV 30) causes attenuated ApopTag labeling compared to untreated and saline-treated animals. Scale bars represent 75 µm. (C) Analysis of images (like those shown in panel B) comparing the number of apoptotic neurons on the side ipsilateral vs. contralateral to CX. Pretreatment with VIV 30 (6.45 ± 0.40; n=5; t=6.131;***p<0.001), VIV 20 (20 mg/kg; 10.80 ± 2.98; n=7; t=6.423;***p<0.001), or

FK506 (4.31 ± 0.96; n=4; t=7.30;***$p<0.001$) significantly attenuated deafferentation-induced ApopTag labeling in P7 AVCN neurons 24 hours post-CX. Sal group does not significantly differ from untreated group. One-way ANOVA was used to compare means to untreated group.

Analysis of neuron number showed that pretreatment with the NFAT inhibitor 11R-VIVIT or FK506 significantly attenuates the percent loss of AVCN neurons (Table 1 & Figure 5E). The means in Figure 5E were also compared to 0.0 using a paired t-test to determine if deafferentation-induced neuron death was completely abolished following treatment with NFAT inhibitor. Loss of AVCN neurons following pretreatment with VIV or FK506 was significantly different from 0.0, indicating that the NFAT activation does not account for the total amount of neuron death following deafferentation. Thus, deafferentation-induced death of AVCN neurons is partly mediated by NFAT.

NFAT regulation of FASL

CaN-dependent activation of NFAT has been shown to result in upregulation of the death receptor ligand FASL (Holtz-Heppelmann et al., 1998; Jayanthi et al., 2005). FASL binds to its receptor FAS to trigger an apoptotic death cascade (Suda and Nagata, 1994) that results in cleavage of DNA which is detected by ApopTag-TUNEL labeling. To determine if deafferentation-induced activation of NFATc4 and subsequent apoptosis of AVCN neurons is linked to the FAS/FASL death pathway, we examined the expression of FASL following deafferentation at P7 when the

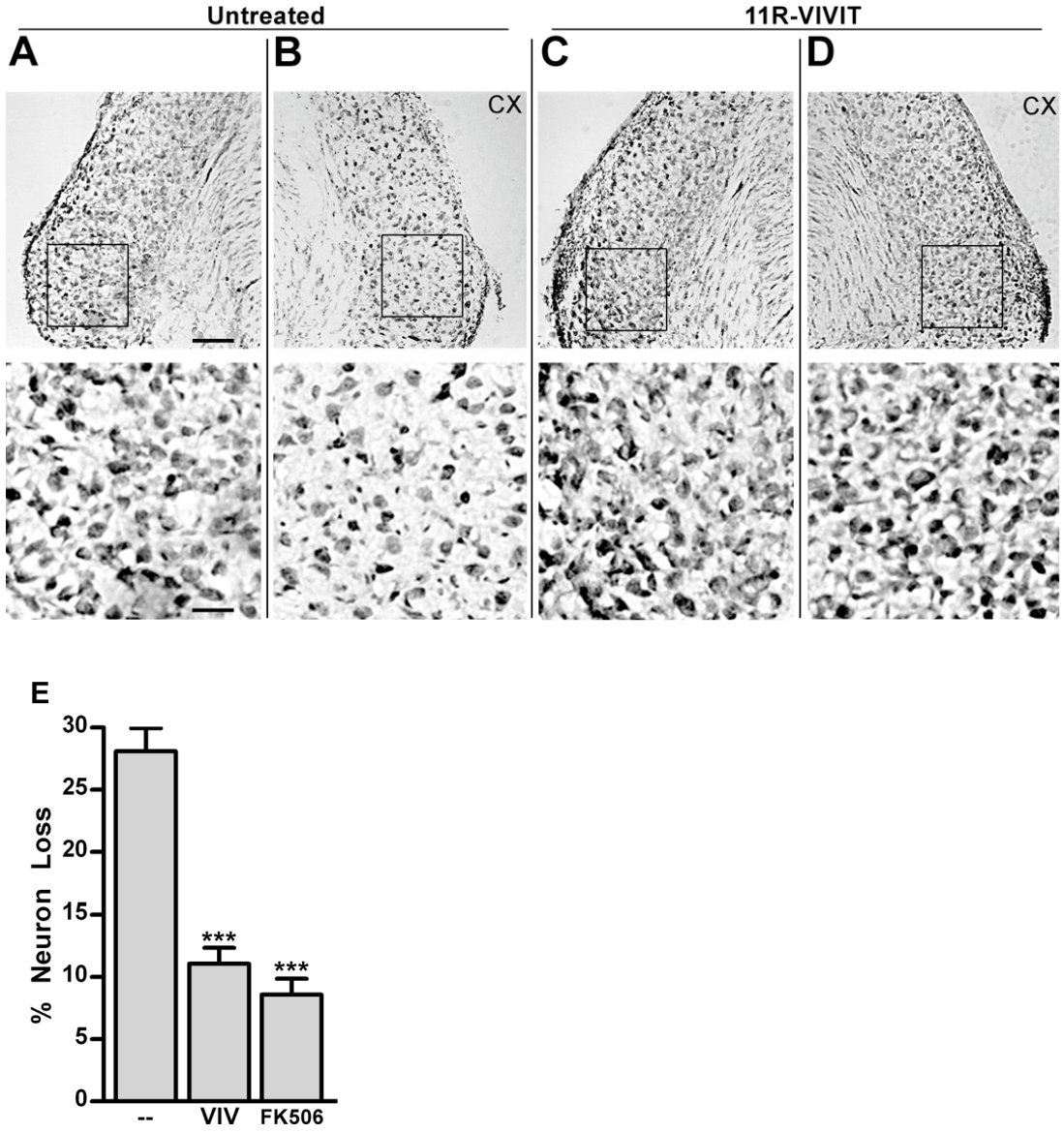

Figure 5. Neuron loss in the AVCN is partly dependent on activation of NFAT. (A-E) Cresyl violet stained sections of AVCN at age P7 show that neuron number is greater in the intact AVCN (A) compared to deafferented AVCN that has undergone 96 hour deafferentation (CX) (B). (C&D) Pretreatment with 30 mg/kg 11R-VIVIT results in no visible difference in neuron number between the intact AVCN (C) and the 96 hour CX AVCN (D). The boxed region in the upper half of panels A-D is

enlarged and shown in the lower half of each panel (scale bar in upper half of panel A represents 140 μm for all upper images; scale bar in lower half of panel A represents 35 μm for all enlarged images). (E) Analysis of images like those shown in panels A-D. The percent neuron loss at age P7 is significantly attenuated compared to the untreated group (--) with VIV pretreatment (30 mg/kg, 11.08 ± 0.91; t=9.42; ***p<0.001), or FK506 (8.00 ± 1.41; t=11.12; ***p<0.001; means compared to – group with one-way ANOVA). Neuron loss was not completely abolished with VIV or FK506 pretreatment (means compared to 0.0 with paired t-test (respectively, t=12.13, **p<0.01; t=5.67, *p<0.05).

cochlear nucleus neurons are susceptible to deafferentation-induced apoptosis. Following 1-hour deafferentation, the fold change of *fasl* mRNA expression in deafferented cochlear nuclei versus intact cochlear nuclei at P7 was measured with semi-quantitative RT-PCR. In untreated mice, *fasl* mRNA expression was significantly increased following deafferentation in both untreated and saline treated animals. Pretreatment with VIV or FK506 eliminated the deafferentation-induced increase of *fasl* mRNA expression (Figure 6A). Figure 6B compares the fold-change in expression of *fas* and *fasl* following deafferentation to ensure that the effect of deafferentation on *fasl* expression is specific and not generally affecting transcriptional regulation. There was no change in *fas* expression following deafferentation demonstrating that the effect of deafferentation was indeed specific. In addition to using *gapdh* as a housekeeping gene, two additional commonly used housekeeping genes (*s15* and *rpl3*) were used in order to confirm the validity of *gapdh* as a control and eliminate the possibility of an artifact-induced effect on *fasl*

expression. Even with the use of alternative housekeeping genes, there was a significant increase in *fasl* expression following deafferentation. Similarly, FASL protein expression was measured 6 hours following deafferentation at P7 with Western blot analysis as shown in Figure 6C. Lanes 1-4 represent the non-deafferented cochlear nucleus tissue lysate from four separate animals and lanes 5-8 represent the corresponding cochlear nucleus tissue lysates from AVCN that were deafferented for 6 hours (Lanes 1 & 5 are from the same animal, as well as 2 & 6, 3 & 7, and 4 & 8; Figure 6C). The analyzed Western blot data are levels of FASL protein represented as ratios of deafferented to control levels. There was a significant increase in FASL protein expression following deafferentation in both untreated and saline treated animals (Figure 6D). Blockade of NFAT activation by pretreatment with 30 mg/kg VIVIT abolished the deafferentation-induced increase of FASL protein *in vivo* (Figure 6D). Together these data indicate that deafferentation induces NFAT-mediated transcription and subsequent translation of FASL. Furthermore, this suggests that the FAS/FASL death pathway may play a role in NFAT-mediated apoptosis of deafferented AVCN neurons during the critical period when they are vulnerable to death.

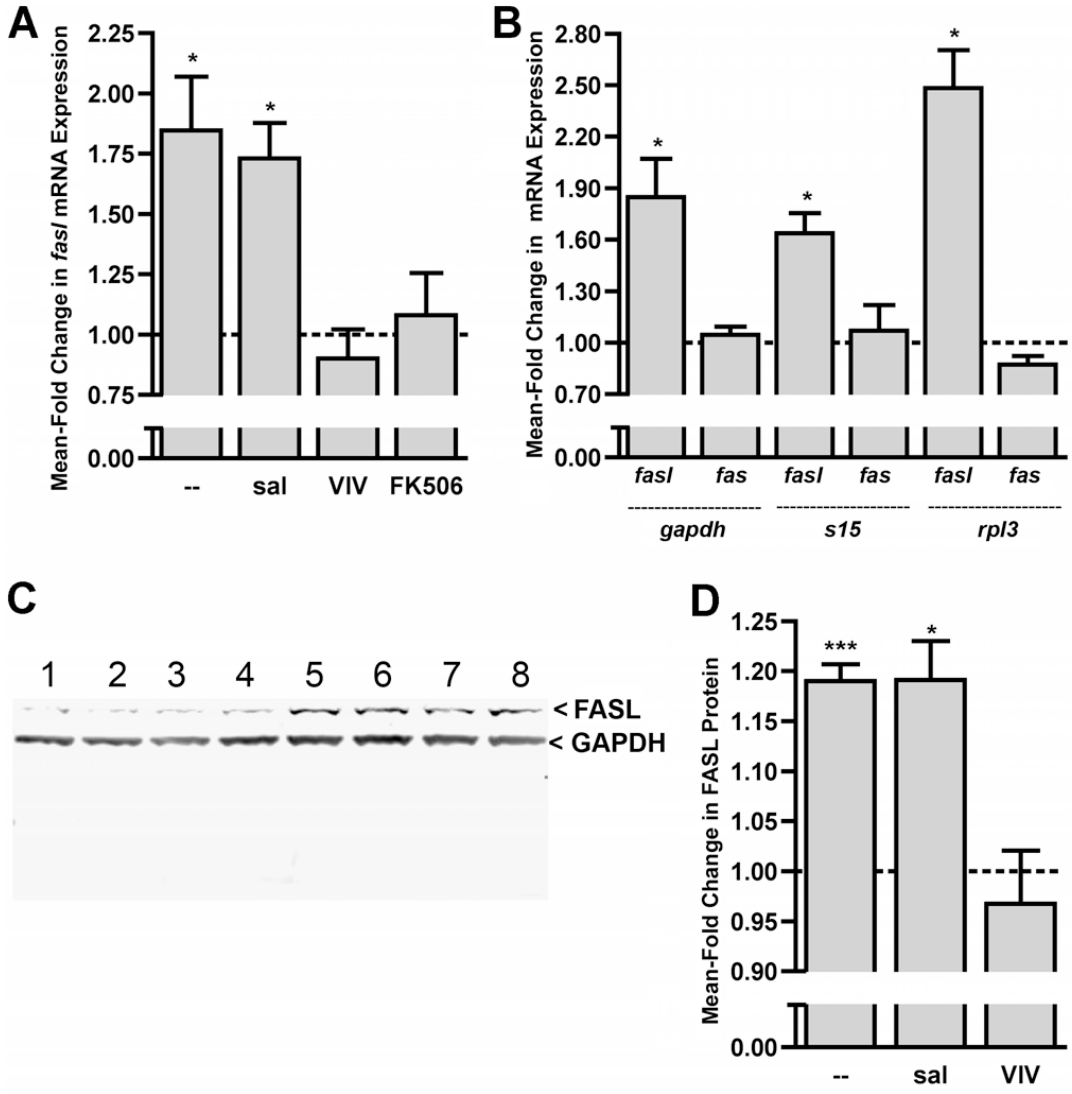

Figure 6. Expression of FASL follows activation of NFATc4 and may play a role in deafferentation-induced NFAT-dependent apoptosis during a critical period of development. (A) Data were obtained by semi-quantitative RT-PCR. At P7 *fasl* mRNA expression is significantly increased 1 hour after deafferentation (CX) in normal (1.85 ± 0.22; n=4; t=3.81; *p<0.05) and saline treated animals (1.73 ± 0.15; n=3; t=4.93, *p<0.05). Pretreatment with VIV (30 mg/kg) or FK506 attenuated the increase of *fasl* mRNA following CX. Means compared to 1.0 with paired t-tests. (B) Semi-quantitative RT-PCR

for both *fas* and *fasl* demonstrating the specificity of CX-induced effects on gene transcription. The housekeeping genes *s15* and *rpl3* were used in addition to *gapdh* to ensure that CX is not affecting the loading control. There was no significant mean-fold change in *fas* expression. The mean fold-change of *fasl* expression remained significant regardless of the housekeeping gene (*gapdh*, 1.85 ± 0.22, t=3.81, *p<0.05; *s15*, 1.64 ± 0.12, t=5.46, *p<0.05; *rpl3*, 2.48 ± 0.22, t=6.71, *p<0.05). Means compared to 1.0 with paried t-tests. (C) FASL protein expression was measured following 6 hour CX at P7 with Western blot analysis. Western blot of non-deafferented cochlear nucleus tissue (lanes 1-4) and 6 hour CX cochlear nucleus tissue (lanes 5-8) are shown and demonstrate increased FASL protein in the deafferented samples. (D) Analysis of Western blots of FASL protein show increased levels of FASL protein in untreated (Fold-change 1.20 ± 0.07; n=7; t=11.0; ***p<0.0001) and saline-treated animals (t=4.9; *p<0.05) following 6 hour CX. Pretreatment with VIV attenuated the increase in FASL protein. With paired t-tests means were compared to 1.0, which represents no change of expression.

Discussion

The susceptibility of AVCN neurons to deafferentation-induced death occurs during a short span of time during development, referred to here and in former studies as a critical period (Tierney et al., 1997; Mostafapour et al., 2000). Consistent with that reported by Mostafapour et al. (2000), we have shown that mice at age P7 are within this critical period, however, by age P14 and certainly P21 the critical period is over and the survival of the neurons is no longer dependent on afferent input from the eighth cranial nerve. It is not known what differentiates AVCN neurons during the critical period from those outside of the critical period. The transcription factor NFATc4 is expressed in AVCN neurons both during and after the critical period. However, its activation occurs exclusively following deafferentation during the critical period (P7) and not after (P14 and P21). We show that the activation/nuclear translocation of NFATc4 following deafferentation of AVCN neurons is rapid (by 15 minutes) and lasts for up to 45 minutes by immunohistochemical analysis. In contrast, our Western blots of fractionated lysates show that NFATc4 remains in the nucleus for less than 30 minutes. This is likely due to an overall reduced detection of NFATc4 in the AVCN when analyzed by Western blot because of the inclusion of additional cell types (i.e. glial cells, which do not express NFATc4), whereas only the AVCN neurons were considered for immunohistochemical analysis.

During the critical period of deafferentation-induced death of AVCN neurons, activation of NFATc4 coincides with susceptibility to apoptosis as well as loss of

neurons. Furthermore, inhibition of NFAT indicates that apoptosis and death of AVCN neurons during the critical period is significantly, although not entirely, dependent on the activation of NFAT. Even so, these data indicate that the mechanism through which NFATc4 is activated during the critical period may characterize, at least in part, what defines their susceptibility to deafferentation-induced death. Since activation of NFATc4 is a calcium-mediated event, there may be differences in calcium signaling or buffering following deafferentation during the critical period versus outside of the critical period.

NFAT proteins are specialized for sensing and responding to dynamic changes in intracellular calcium concentration because of their ability to rapidly translocate to and from the nucleus via the opposing activities of CaN and kinases (Loh et al., 1996). As soon as one minute following either a high but short, or low but sustained increase in intracellular calcium concentration, NFAT can become activated and remain activated for several minutes following stimulation (Dolmetsch et al., 1997). Therefore, the nature of the deafferentation-induced calcium signal remains to be determined in terms of duration, magnitude, and origin. The time-course of NFATc4 activation necessary for NFAT-mediated transcription in neurons observed here is similar to a previous result reporting stimulation-induced (depolarization with 90 mM potassium) nuclear translocation of NFATc4 in hippocampal neurons by 15 minutes with a duration of at least 60 minutes (but less than 120 minutes), and subsequent NFATc4-dependent gene transcription (Graef et al., 1999). This is similar to our results in that we also show rapid activation of NFATc4 by 15 minutes following

deafferentation. The duration of NFATc4 activation in our system is shorter (lasting 45 minutes rather than 60-120 minutes), however, our observations were made in a unique population of cells, *in vivo,* and under a different stimulus paradigm. While it may seem paradoxical that NFATc4 activation in hippocampal neurons is stimulus-dependent and the activation of NFATc4 in AVCN neurons occurs following deafferentation, one must remember that in addition to source, important parameters dictating the effect of a calcium signal include duration, magnitude and physical location (Franks and Sejnowski, 2002): all of which may be similar or variable in the two experimental systems, but obviously combine to result in a CaN/NFATc4 activating signal. *In vivo* deactivation of NFATc4 in AVCN neurons may be a more rapid process than that observed in cultured hippocampal neurons. Inhibition of NFAT resulted in inhibition of *fasl* transcript and protein expression, demonstrating that activation of NFATc4 for 45 minutes is sufficient to mediate the expression of *fasl* in AVCN neurons.

Genes transcribed by activated NFATc4 may lead to the eventual death of a subpopulation of deafferented AVCN neurons. Considering that FASL expression has been shown to be dependent on NFAT activation (Holtz-Heppelmann et al., 1998; Jayanthi et al., 2005), and that FASL expression initiates an apoptotic pathway (Suda and Nagata, 1994; Raoul et al., 1999; Raoul et al., 2002), FASL is a good candidate for involvement in the mechanism of deafferentation-induced AVCN neuronal death. While it is interesting to note that cell death in deafferented *avian* cochlear nucleus does not depend upon changes in gene transcription (Garden et al., 1995), it is

difficult to make comparisons with the mechanisms of deafferentation-induced death in AVCN due to the incomplete understanding of the specific mechanisms underlying the death in either system. The presence and/or expression levels of NFATc4, FAS, and FASL are unknown in chick cochlear nucleus under normal conditions as well as after deafferentation. Further studies are required to make a sound comparison between mechanisms of deafferentation-induced neuronal death in avian and murine cochlear nuclei.

Here, NFAT regulates the expression of FASL in AVCN neurons as indicated by the blockade of FASL expression when NFAT activation is specifically inhibited with 11R-VIVIT. Additionally, apoptosis of deafferented AVCN neurons is shown to be partly dependent upon activation of NFAT as suggested by the significant attenuation of apoptosis following inhibition of NFAT activation. One mechanism by which upregulation of FASL can result in deafferentation-induced death of AVCN neurons is by inserting into the cell membrane and binding to its receptor FAS, expressed on the membranes of adjacent neurons, subsequently triggering apoptosis in the FAS expressing neurons. This is a potential mechanism, as FAS is endogenously expressed in mammalian cochlear nucleus tissue (Guan et al., 2005) although its expression pattern in the cochlear nuclei of mice has not yet been characterized in detail. The level of expression of FASL may be the limiting factor that regulates the induction of apoptosis in AVCN neurons, which depends upon activation of NFAT. Note that we hypothesize that the AVCN neurons with activated NFATc4 following deafferentation are not the neurons that die, but the neurons that

induce death in neighboring neurons that express FAS. Consistent with this hypothesis is the finding that deafferentation leads to CREB activation in the surviving auditory neurons (Zirpel et al., 2000a). This also parallels the hypthothesis that CREB leads to the expression of AP-1, which then partners with activated NFAT to induce FASL expression and subsequent initiation of FAS-dependent apoptosis in adjacent neurons. It would be interesting to determine if deafferentation induces both NFAT and CREB activation in the same population of auditory neurons.

Previous research on the proto-oncogene BCL-2 supports our finding that NFAT-mediated expression of FASL following deafferentation is a likely contributor to the deafferentation-induced apoptosis of AVCN neurons as this hypothesis fits logically into previous studies that examine BCL-2 not only in the context of the FAS/FASL death pathway but also in the context of activity-dependent survival of neurons in the auditory system. BCL-2 is an anti-apoptotic protein that significantly inhibits FAS/FASL-mediated cell death (Itoh et al., 1993). In addition, BCL-2 inhibits apoptosis induced by NFAT-mediated expression of FASL (Srivastava et al., 1999). Interestingly, over-expression of BCL-2 eliminated neuron death of deafferented AVCN during the critical period (Mostafapour et al., 2002). This implies that BCL-2 may be inhibiting the upregulation of FASL expression that follows deafferentation of AVCN neurons that are beyond the critical period, ultimately preventing their death by suppressing the FAS/FASL apoptotic pathway. Similarly, Harris et al. (2005) found, using microarray analysis, that AVCN from mice within the critical period express higher levels of transcript for pro-apoptotic

genes than AVCN from mice beyond the critical period, and conversely, AVCN from mice beyond the critical period express higher levels of transcript for pro-survival genes than AVCN from mice within the critical period. This indicates a developmental "switch" in AVCN from a complement of cellular mechanisms favoring induction of an apoptotic pathway, to a complement of mechanisms that prevent, or eliminate apoptotic pathways. Our data are consistent with this and suggest that NFAT may, in part, be a molecular mechanism underlying this developmental switch.

Figure 7 is a schematic model of our hypothesis for deafferentation-induced apoptosis of cochlear nucleus neurons during the developmental critical period for activity-dependent survival. This hypothesis is consistent with the data presented in the current study as well as in previous reports. Deafferenation leads to an increase in intracellular calcium concentration that binds to and activates CaM. Calcium/CaM then binds to CaN leading to rapid dephosphorylation, activation and nuclear translocation of NFATc4 as shown by this study (Figures 2, 3, & 4). Activated/nuclear NFAT then induces expression of the death receptor ligand FASL (Figure 6), which contributes to the death of deafferented cochlear nucleus neurons by triggering the apoptotic death cascade (Figures 1, 4, & 5) in neurons that express, either endogenously or deafferentation-induced, the death receptor FAS, perhaps only during the critical period. This is shown as a calcium-mediated process because inhibition of NFAT activation specifically via the calcium-mediated pathway eliminates increased FASL expression and attenuates neuronal death *in vivo*. The

events shown in Figure 7 that occur following deafferentation and up to the point of FASL expression have been shown in the current study or previously; the events beyond this point that show the presence of FAS receptors on neighboring neurons and their activation-dependent apoptosis need to be studied further.

Classically, the role of NFAT is described in the context of lymphocyte function and its role in the immune system. Alternatively, this study provides an example of a role for NFAT in the plasticity of the nervous system, a role that is becoming more common (Groth and Mermelstein, 2003; Hernandez-Ochoa et al., 2006). In summary, we have shown that NFATc4 is activated following deafferentation, and that this event leads to increased FASL expression and apoptosis of cochlear nucleus neurons. This study presents convincing evidence for the involvement of NFAT in deafferentation-induced apoptosis of AVCN neurons, but the specific cellular pathways remain to be elucidated. Regardless, this research provides a novel mechanism through which deafferentation-induced death of AVCN neurons, and possibly other types of sensory neurons, may occur.

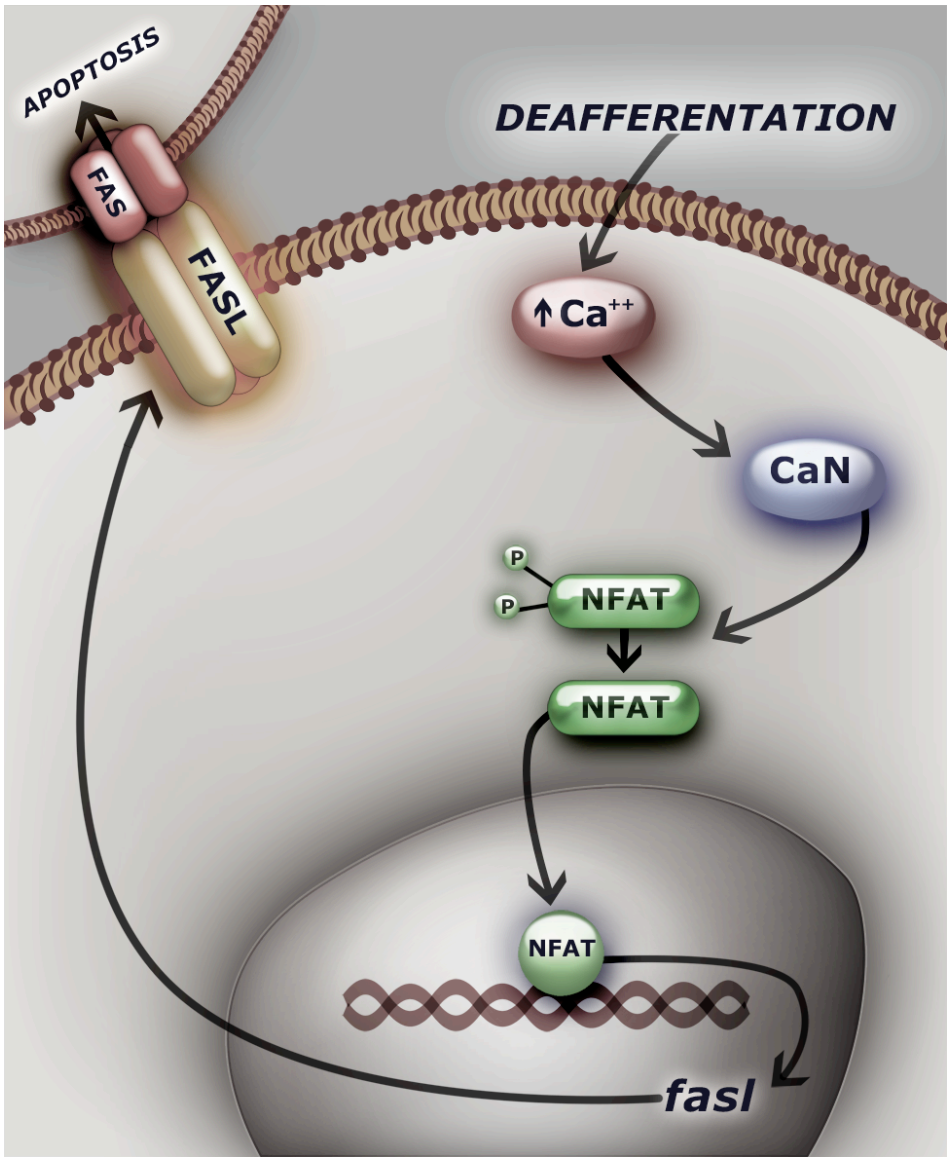

Figure 7. A proposed model for deafferentation-induced apoptosis of cochlear nucleus neurons during a developmental critical period. Following deafferentation, NFATc4 is activated by Ca/CaM/CaN and translocates to the nucleus where it mediates transcription and translation of the death receptor ligand FASL. We hypothesize that upregulation of FASL expression results in apoptosis of adjacent neurons that express the death receptor FAS.

Importantly, the data here have also provided a strategy for reducing neuron death following deafferentation. Namely, treatment with the cell-permeable peptide 11R-VIVIT, which specifically blocks NFAT activation, significantly reduced auditory neuron death following deafferentation. This and other strategies for interfering with the novel pathway shown here may be useful for rescuing deafferented auditory neurons from death. This has important implications for increasing the effectiveness of cochlear implant devices, which require functional neurons in order to be successful at restoring hearing.

Chapter Three

Progesterone Inhibition of Voltage-Gated Calcium Channels as a Potential Neuroprotective Mechanism Against Excitotoxicity

Introduction

Progesterone has been well studied regarding its role in reproductive processes acting via the intracellular progestin preceptor. In addition, concentrations of progesterone in excess of that required to activate its cognate receptor are neuroprotective following a variety of insults, including impact injury, ischemia, and excitotoxicity (Goss et al., 2003; Robertson et al., 2006; Sayeed et al., 2006; Wright et al., 2007; Xiao et al., 2008; Atif et al., 2009). As such, progesterone has reached phase III clinical trials as a therapeutic treatment following traumatic brain injury (Vandromme et al., 2008; Wright, 2010). Although the neuroprotective effects of progesterone have been well characterized, the underlying molecular mechanisms remain undetermined.

Neuronal death following brain injury can be a complex process involving many factors (Globus et al., 1995; Arundine and Tymianski, 2004; Atif et al., 2009). One principal form of excitotoxicity is glutamate-induced calcium overload (Choi, 1985; Tymianski and Tator, 1996; Bender et al., 2009; Xu et al., 2009; Schauwecker, 2010; Szydlowska and Tymianski, 2010). Activation of glutamate receptors may directly lead to calcium influx, but with prolonged depolarization, additional sources of calcium are recruited, notably the activation of voltage-gated calcium channels (Figure 1). These secondary sources of calcium strongly contribute to calcium overload, and thus also have an essential role in excitotoxicity. As such, progesterone inhibition of either glutamate receptors or voltage-gated calcium channels would be

neuroprotective. Inhibition of one calcium channel subtype in particular, the L-type calcium channel, would be particularly effective, as pharmacological block of this channel following the induction of excitotoxicity is highly neuroprotective (Miyazaki et al., 1999; Vallazza-Deschamps et al., 2005; Sribnick et al., 2009).

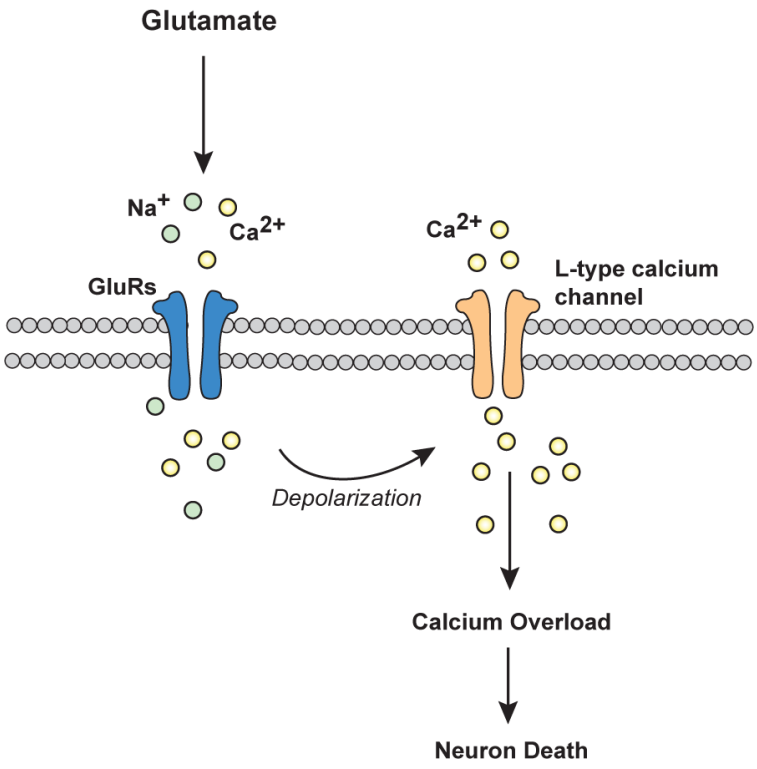

Figure 1. A putative pathway for excitotoxicity. Prolonged stimulation of ionotropic glutamate receptors leads to an influx of sodium and calcium ions that results in neuron depolarization. Consequently, voltage-gated L-type calcium channels are activated to allow calcium influx and subsequent initiation of death pathways.

The activation of L-type calcium channels may contribute to excitotoxicity through its privileged role in regulating a number of activity-dependent transcription factors, including nuclear factor of activated T-cells (NFAT) and cAMP response-element binding protein (CREB) (Deisseroth et al., 2003; Weick et al., 2005). For example, NFAT activation can initiate cell death by way of increasing expression of the ligand FASL (Rao et al., 1997; Kondo et al., 2003; Jayanthi et al., 2005; Flockhart et al., 2008; Luoma and Zirpel, 2008). Interestingly, while CREB is well known for its role in pro-survival mechanisms (reviewed in (Walton and Dragunow, 2000; Kinjo et al., 2005)), CREB may also facilitate cellular death by way of its ability to induce the expression of transcription factor complex activator protein 1 (AP-1). This is due to the fact that AP-1 partners with NFAT to mediate transcription of FASL (Macian et al., 2000). The coordinated changes in the activity of these and other calcium sensitive transcription factors may ultimately determine the fate of a neuron following traumatic brain injury.

The striatum is a brain region in which the neuroprotective effects of progesterone have been previously demonstrated (Ozacmak and Sayan, 2009). In this study we utilized cultured striatal neurons to uncover the potential mechanisms behind the neuroprotective effects of progesterone. This model system offers several advantages for studying neurotoxicity. First, striatal neurons in culture lack glutamatergic input. Thus, while these neurons are sensitive to glutamate agonists, direct depolarization does not evoke appreciable glutamate release, allowing for the

isolation of primary and secondary mechanisms of excitotoxicity. Second, cultured neurons offer excellent access for genetic and pharmacological manipulation as well as for electrophysiological and optical measurements. As described below, we found therapeutic concentrations (i.e. micromolar) of progesterone to be neuroprotective against excitotoxicity. Furthermore, progesterone acted by blocking voltage-gated calcium currents in a concentration-dependent manner, resulting in an inhibition of L-type calcium channel-dependent gene expression. The effects on L-type calcium channel-dependent gene expression were specific to progesterone; other progestins as well as other classes of steroid hormones were without effect. In addition, the actions of progesterone occurred at the neuronal membrane, were not sex-specific nor did they appear to be progestin receptor mediated. Progesterone did not inhibit AMPA or NMDA receptor-mediated glutamatergic signaling, indicating the actions of the steroid were specific to the secondary mechanisms of excitotoxicity. Overall, these data provide greater insight into the neuroprotective actions of progesterone, and support the potential use of progesterone for neuroprotection across various paradigms.

Materials and Methods

Cell Culture

Striatal neurons were cultured from P0-P1 Sprague-Dawley rats as previously described (Mermelstein et al., 2000), using a protocol approved by the by the Animal Care and Use Committee at the University of Minnesota. The effects of progesterone reported here did not differ between cultures derived solely from males or females. Chemicals are from Sigma (St. Louis, MO) unless noted otherwise. Following decapitation, striatal neurons were isolated in ice-cold HBSS (pH 7.35, 300 mOsm) containing 4.2 mM $NaHCO_3$, 1mM HEPES, and 20% fetal bovine serum (FBS; Hyclone, Logan, UT). Tissue was washed and digested for 5 minutes in trypsin solution (type XI, 10 mg/ml) containing (in mM): 137 NaCl, 5 KCl, 7 Na2HPO4, and 25 HEPES, with 1500 U of DNase, pH 7.2, 300 mOsm. Following wash with HBSS with 20% FBS, dissociation of the tissue was performed using Pasteur pipettes of decreasing diameters. The dissociated cells were pelleted twice to remove contaminants, plated on 10 mm coverslips (treated with Matrigel for adherence; BD Biosciences, San Jose, CA) and incubated at room temperature for 15 minutes. One ml of minimum essential medium (MEM; Invitrogen, Grand Island, NY) with 28 mM glucose, 2.4 mM $NaHCO_3$, 0.0013 mM transferrin (Calbiochem, La Jolle, CA), 2 mM glutamine, and 0.0042 mM insulin with 1% B-27 supplement (Invitrogen) and 10% FBS, pH 7.35, 300 mOsm was added to each coverslip containing well. To stunt glial growth, 1 ml of medium containing cytosine (4 μM) 1-β-D-arabinofuranoside and 5%

FBS was added 24-48 hours after plating. Four or five days later, 1 ml of medium was replaced with modified MEM containing 5% FBS.

Drugs

Drugs used are as follows: tetrodotoxin (500 nM; TTX; Tocris, Ellisville, MO); glutamic acid (3 μM; glutamate; Sigma); Pregn-4-ene-3,20-dione (100 nM-100 μM, see Results; progesterone; Sigma); 5-Cholesten-3β-ol (50 μM; cholesterol; Sigma); 1,4-Dihydro-2,6-dimethyl-4-(2-nitrophenyl)-3,5-pyridine dicarboxylic acid dimethyl ester (5 μM; nifedipine; Tocris); 17β-Estradiol (50 μM; estradiol; Sigma); 11β,21-Dihydroxyprogesterone (50 μM; corticosterone; Sigma); 5α-Androstan-7β-ol-3-one (50 μM; dihydrotestosterone; Steraloids, Newport, RI); 3β-Hydroxy-5α-pregnan-20-one acetate (50 μM; allopregnanolone; Sigma); (3a,5b)-3-Hydroxy-pregnan-20-one (50 μM; pregnenolone; Tocris).

Cell Death Assay

Striatal neurons cultured on 10 mm coverslips were washed twice with Tyrode's solution and then incubated in either Tyrode's solution or Tyrode's solution containing 60 mM KCl (60K; an equimolar concentration of NaCl was subtracted to maintain osmolality) for 3 hours at room temperature. The cells were then fixed for 15 minutes with ice-cold 4% paraformaldehyde in PBS. After fixation, apoptotic cells were identified using ApopTag Fluorescein *In Situ* Apoptosis Detection Kit (Chemicon). Product protocols were followed exactly. All cells were counterstained

by use of a mounting medium containing DAPI; Prolong antifade with DAPI (Invitrogen; Carlsbad, CA). As a positive control, sections were pretreated with DNase buffer (30 mM Trizma, pH 7.2, 4 mM $MgCl_2$, 0.1 mM dithiothreitol (DTT)) for 5 minutes at RT, DNase I (1000U/ml; Invitrogen) for 10 minutes at RT, and 5×3 minute PBS washes before proceeding with the protocol. This resulted in ApopTag labeling of nearly all cells. As a negative control, TdT (terminal deoxynucleotidyl transferase) was replaced with PBS, which resulted in no labeled cells.

Fluorescently labeled cells were visualized with a Leica DM4000B microscope (Leica Microsystems; Wetzlar, Germany) using a 40X air objective and filter sets for FITC and DAPI imaging. Images were acquired with a Leica DFC 500 camera and Lecia Application Suite v3.3 software. Images were analyzed using Adobe Photoshop. The total number of neurons and the apoptotic number of neurons were counted in three fields of view per coverslip. Neurons were discerned from glia based on morphology. The percentage of apoptotic or dying neurons was then calculated for each field of view. Data are reported as the mean ± SEM. All groups were compared to the control or Tyrode's solution treatment group using paired t-tests.

Calcium Imaging

Coverslips were washed in standard buffer (SB); (in mM) 130 NaCl, 5.4 KCl, 2.5 $CaCl_2$, 1.5 $MgCl_2$, 10 HEPES, 20 Glucose, 0.01 Glycine with TTX (500 nM), pH 7.4, 300 mOsm. Cells were then incubated in Fluo-4 AM calcium indicator (1 µM; Molecular Probes; Eugene, OR) diluted in SB at 37ºC for 45 minutes followed by 15

minute wash in SB at RT. The coverslip was then placed into a bath chamber and cells were visualized through a 10X objective on an Olympus IX70 inverted microscope (Olympus Corporation, Tokyo, Japan) with attached ORCA-ER camera (Hamamatsu Photonics K.K., Hamamatsu, Shizuoka, Japan). Images were acquired using Metamorph software (Molecular Devices, Silicon Valley, CA) every 2 seconds. A Xe-arc lamp was used as a light source. The following optical filters were used: beam-splitter = 495 nm, excitation = 470 ± 20 nm, and emission = 525 ± 25 nm. Images were collected during a 60 second wash with SB, 30 second stimulation (with SB containing either 20 mM KCl (20K) or 3 μM glutamate; for 20K an equimolar concentration of NaCl was decreased to maintain osmolality) and 90 second wash with SB. This imaging sequence was repeated three times with a 13.5 minute pause between each series, for a total inter-stimulus interval of 15 minutes. In experiments where the effect of a drug was tested, the second series differed in that the initial 60 second wash was replaced by a 30 second wash in SB followed by 30 second application of drug in SB and then followed by 30 second stimulation including drug. Images were analyzed using Image J 1.43 (Rasband, W.S., ImageJ, U.S. National Institutes of Health, Bethesda, Maryland, USA, http://rsb.info.nig.gov.ij/). At least 100 cells were analyzed for each experiment. Cell intensity was normalized to baseline fluorescence at the start of image acquisition. The maximum intensity of the second and third stimulations was normalized to that of the first stimulation for each experiment. Significance was determined using paired t-tests.

Electrophysiology

Whole-cell currents were recorded from cultured striatal neurons (7 to 14 d.i.v.) using standard voltage-clamp techniques. All experiments were conducted at room temperature. Recordings were performed using an Axopatch 200B amplifier (Molecular Devices, Foster City, CA), controlled by a personal computer running pClamp software (version 10.2.0.14). All recordings were filtered at 2 kHz, and the series resistance was compensated 40-60%. Holding current and access resistance were monitored during recordings, and experiments with holding currents > 500 pA or unstable access resistance greater than 20 MΩ were excluded from analysis. Recording electrodes were pulled by a Model P-97 Flaming/Brown micropipette puller (Sutter Instrument Co., Novato, CA) to resistances between 2.8 and 5.5 MΩ. The perfusion system consisted of a convergent single-barrel design that allowed for extracellular solution changes in ~1 s. Extracellular solution for AMPA-mediated currents contained the following (mM): 130 NaCl, 5.4 KCl, 2.5 $CaCl_2$, 1.5 $MgCl_2$, 10 HEPES, 20 Glucose, 0.01 Glycine and 0.0005 TTX. Extracellular solution for recording NMDA-mediated currents contained the following (mM): 130 NaCl, 5.4 KCl, 3.9 $CaCl_2$, 0.1 $MgCl_2$, 10 HEPES, 20 Glucose, 0.01 Glycine and 0.0005 TTX. Extracellular solution for recording voltage-gated calcium currents contained the following (mM): 135 NaCl, 20 CsCl, 1 $MgCl_2$, 10 HEPES, 5 $BaCl_2$ and 0.0005 TTX. The intracellular recording solution for measuring AMPA- and NMDA-mediated currents contained the following (in mM): 145 K-gluconate, 10 HEPES, 8 NaCl, 2 ATP, 3 GTP and 0.2 EGTA. The intracellular recording solution for voltage-gated

calcium currents contained the following (in mM): 190 N-methyl-D glucamine, 40 HEPES, 5 BAPTA, 4 $MgCl_2$, 12 phosphocreatine, 3 Na_2ATP, and 0.2 Na_3GTP. Drugs to activate ligand-gated ion channels were applied through an adjacent (~1-200 microM away from the soma) pipette via a Picospritzer (Parker-Hannifin, Cleveland, OH) at a pressure of 10 psi for a duration 200 ms. The Picospritzer was activated by a trigger from the acquisition software. Membrane potential was held at -70 mV for AMPA experiments and -40 mV for NMDA experiments. In voltage-gated ion channel experiments whole-cell currents were activated by a step from -80 mV to 0mV for a period of 100 ms. Data was analyzed in Clampfit 10.2 and Microsoft Excel (Redmond, WA) then plotted using GraphPad Prism 4.0 (La Jolla, CA).

Luciferase Assays

Cultured striatal neurons were transfected at either 7 or 8 d.i.v. with a luciferase-based reporter (0.75 µg/coverslip) of either NFAT- or CRE-dependent transcription using Optifect transfection reagent (1 µl Optifect /coverslip; Invitrogen) per manufacturer's instructions. After transfection the media was replaced with serum-free DMEM (Invitrogen) containing 1% B-27 supplement and 1% insulin-transferrin-selenium supplement (Invitrogen) (DMEM-ITS) and BayK8644 (1 µM) for stabilization of L-type calcium channels (Kim and Usachev, 2009). Cells were incubated at 37ºC in 5% CO_2. In groups to be stimulated, incubation was carried out in DMEM-ITS containing either 20K with or without drug as indicated in results.

Approximately 16 hours later, the cells were lysed and luciferase activity was assayed using a standard luminometer (Monolight 3010; PharMingen, San Diego, CA). Each treatment group had 8-10 coverslips. All experiments were performed three times. Statistical significance between groups was similar in each experiment and was determined by one-way ANOVA with Bonferroni post-hoc ($p < 0.05$).

Results

Progesterone is neuroprotective against excitotoxicity

To recapitualate the *in vivo* findings by others, our first experiment examined the neuroprotective effect of progesterone on cultured striatal neurons following prolonged depolarization. Direct depolarization was achieved by replacing the extracellular bath solution with one containing elevated potassium. Application of 60 mM potassium (60K) for 3 hours in the presence of vehicle (Veh) significantly increased the percent of dying/apoptotic neurons as compared to the non-depolarized controls (Figure 2A). By comparison, progesterone (50 μM) eliminated the 60K-induced increase in neuronal death. As controls for steroid specificity, we also treated neurons with the progesterone metabolite allopregnanolone (50 μM) or the progesterone precursor pregnenalone (50 μM). Neither allopregnanolone nor pregnenalone had any effect on 60K-induced neuronal death. We next determined the importance of L-type calcium channels in depolarization-induced neuron death by applying the L-type calcium channel blocker nifedipine (5 μM). As hypothesized, nifedipine eliminated depolarization-induced cell death (Figure 2B). Following the verification that progesterone is neuroprotective in striatal cultures, the remainder of the studies focused on examining the physiological impact of progesterone following cellular depolarization.

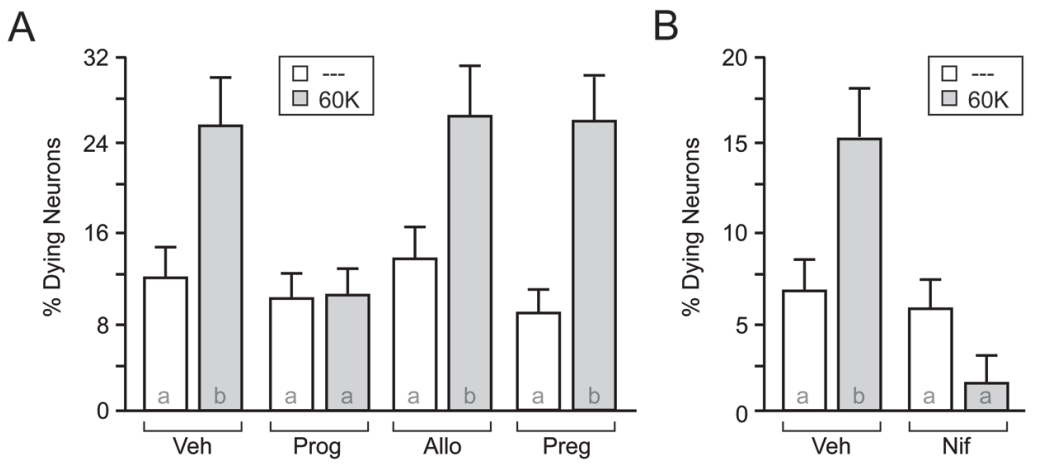

Figure 2. Progesterone blocks depolarization-induced neuronal death. A and B, Graphical representation of depolarization-induced apoptosis in striatal neurons. (A) Application of 60 mM potassium (60K) for 3 hours induced a significant increase in apoptotic neurons ($t = 4.69$; $p < 0.0001$) that was blocked by progesterone (Prog; 50 μM; $t = 0.24$; $p > 0.05$). Pregnenolone (Preg; 50 μM; $t = 3.32$; $p < 0.05$) or Allopregnanolone (Allo; 50 μM; $t = 3.58$; $p < 0.01$) did not affect the induction of apoptosis by 60K. (B) Nifedipine (Nif; 5 μM) blocked 60K-induced apoptosis ($t = 0.28$; $p > 0.05$). Letters in bars represent statistically similar groups as analyzed by a two-tailed one-way ANOVA with Bonferroni post-hoc analysis.

Progesterone inhibits signaling events mediated by voltage-gated calcium channels

As striatal neurons in culture lack intrinsic glutamatergic input, progesterone-mediated neuroprotection following depolarization suggested the steroid could act on secondary forms of calcium entry in models of excitotoxicity. In the next series of experiments, we examined the effect of depolarization on intracellular calcium concentrations in order to determine whether progesterone directly affects voltage-

gated calcium channel signaling. If so, this would provide a putative mechanism for neuroprotection. Alternatively, progesterone could be neuroprotective by affecting processes downstream of the calcium channels. Each experiment consisted of three separate 30-second stimulations with 20 mM potassium (20K)-evoked peaks, separated by approximately 15 minutes. This allowed for the measurement of responses in the presence of a drug (peak 2) relative to control conditions (peak 1) as well as a reversal or 'wash-out' of the drug (peak 3). The maximum value of each response was normalized to the first response to compensate for physiological run-down and photometric bleaching. This experimental design utilized 20K as the stimulus, as this resulted in a consistent, reversible and reproducible increase in intracellular calcium that is predominantly through L-type calcium channels (Mermelstein et al., 2000).

Application of 20K induced a marked increase in intracellular calcium that was not affected by the presence of vehicle (Figure 3A). The majority of the 20K-induced calcium signal was due to the activation of L-type calcium channels, as determined by nifedipine administration (Figure 3B,F). Furthermore, progesterone also significantly reduced the depolarization-induced calcium increase (Figure 3C,F) providing evidence that modulation of calcium channel activity is a possible site of action for progesterone-mediated neuroprotection. As in the neuroprotection assay, allopregnanolone and pregnenalone were ineffective at altering the calcium signal (Figures 3D-F).

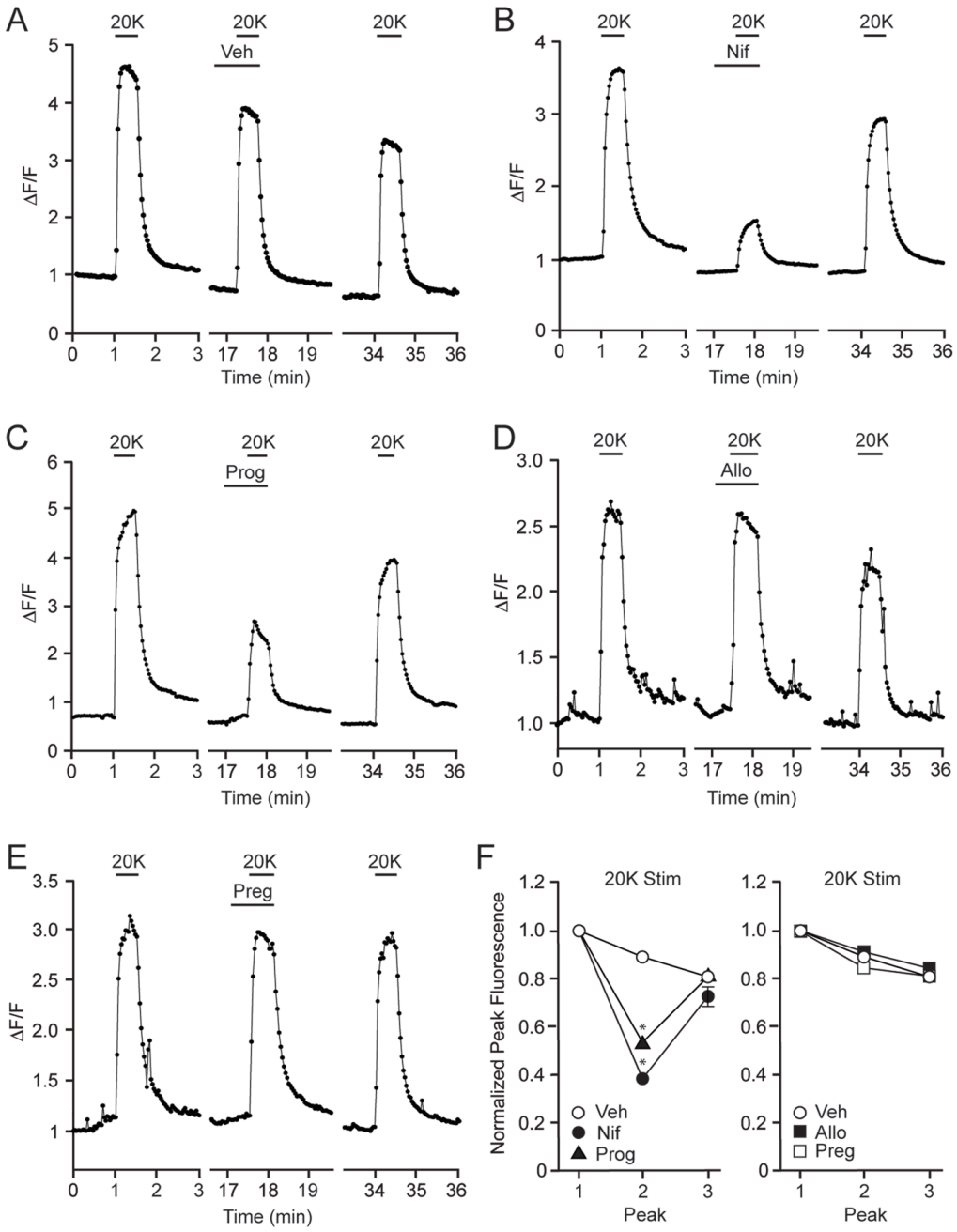

Figure 3. Progesterone attenuates depolarization-induced L-type calcium channel-mediated increase of intracellular calcium. (A) Increases in intracellular calcium following depolarization with 20 mM potassium (20K) in the presence of vehicle (Veh). (B) The 20K-induced increase in intracellular

calcium is primarily through activation of L-type calcium channels, as demonstrated following application of Nif (5 μM). (C-E) Progesterone (50 μM) attenuates the 20K-mediated increase in intracellular calcium, whereas Allo (50 μM) or Preg (50 μM) is without effect. (F) Summarized data. 20K-induced calcium signals were largely attributable to activation of L-type calcium channels ($t = 12.25$; $p < 0.05$). The actions of 20K were also attenuated by Prog ($t = 7.64$; $p < 0.05$) but not Allo ($t = 0.72$; $p > 0.05$) or Preg ($t = 0.10$; $p > 0.05$).

Following the observation that progesterone inhibits the increase in intracellular calcium from direct depolarization, and previous work showing modulation of calcium currents in smooth muscle cells with parallel concentrations of progesterone (Bielefeldt et al., 1996), we sought to determine how progesterone affected whole-cell currents associated with voltage-gated calcium channels. Using Ba^{2+} as the charge carrier, inward currents were evoked by a step depolarization from -80 to 0 mV. In the presence of progesterone, I_{Ba} was inhibited 67 ± 3% (Figure 4A). This block represents a voltage-gated calcium current far in excess of the ~30% carried by striatal L-type calcium channels (Bargas et al., 1994). The inhibition of I_{Ba} was stable by the end of a 1 minute application, and was readily reversible (Figure 4B). The IC_{50} of progesterone-mediated inhibition of I_{Ba} was 27 μM (Figure 4C). Furthermore, at the highest concentration tested (100 μM), progesterone completely blocked the whole-cell current indicating widespread effects of progesterone across all voltage-gated calcium channel subtypes. To identify the location of action of progesterone-mediated inhibition of calcium channel activity, we measured the same

currents with progesterone (50 μM) added to the internal pipette solution. Dialysis of the cell with progesterone had no effect on whole-cell calcium current size: 425 ± 79 pA versus 573 ± 123 pA in vehicle-matched controls ($n \geq 7$ in each group). In these same experiments, the equivalent concentration of progesterone (50 μM) was applied in the extracellular solution. External application of progesterone to the progesterone dialyzed cells still resulted in a progesterone-mediated inhibition of I_{Ba} by 64 ± 7%. These results indicate that progesterone blocks calcium channels by acting at the external surface of the plasma membrane, independent of classical steroid hormone receptor signaling (see discussion). As in previous experiments, allopregnanolone and pregnenalone were tested for similar effects. Neither steroid showed notable inhibition of I_{Ba} (Figure 4D). Taken together, these results show that progesterone inhibits voltage-gated calcium channels in a reversible, concentration-dependent and steroid-specific manner, acting at the plasma membrane.

Progesterone blocks activation of calcium-dependent gene expression

With progesterone able to inhibit voltage-gated calcium channel function, we next sought to verify that progesterone would inhibit activity-dependent transcription. Consistent with previous results (Weick et al., 2003; Groth et al., 2008), 20K-mediated depolarization significantly increased NFAT-dependent transcription in striatal neurons (Figure 4A). In parallel with its actions on L-type calcium channels, progesterone at 50 μM completely abolished 20K-induced NFAT-dependent

transcription (Figure 4A,B). Progesterone inhibited NFAT-dependent transcription in a concentration-dependent manner (IC_{50} = 5.2μM, data not shown).

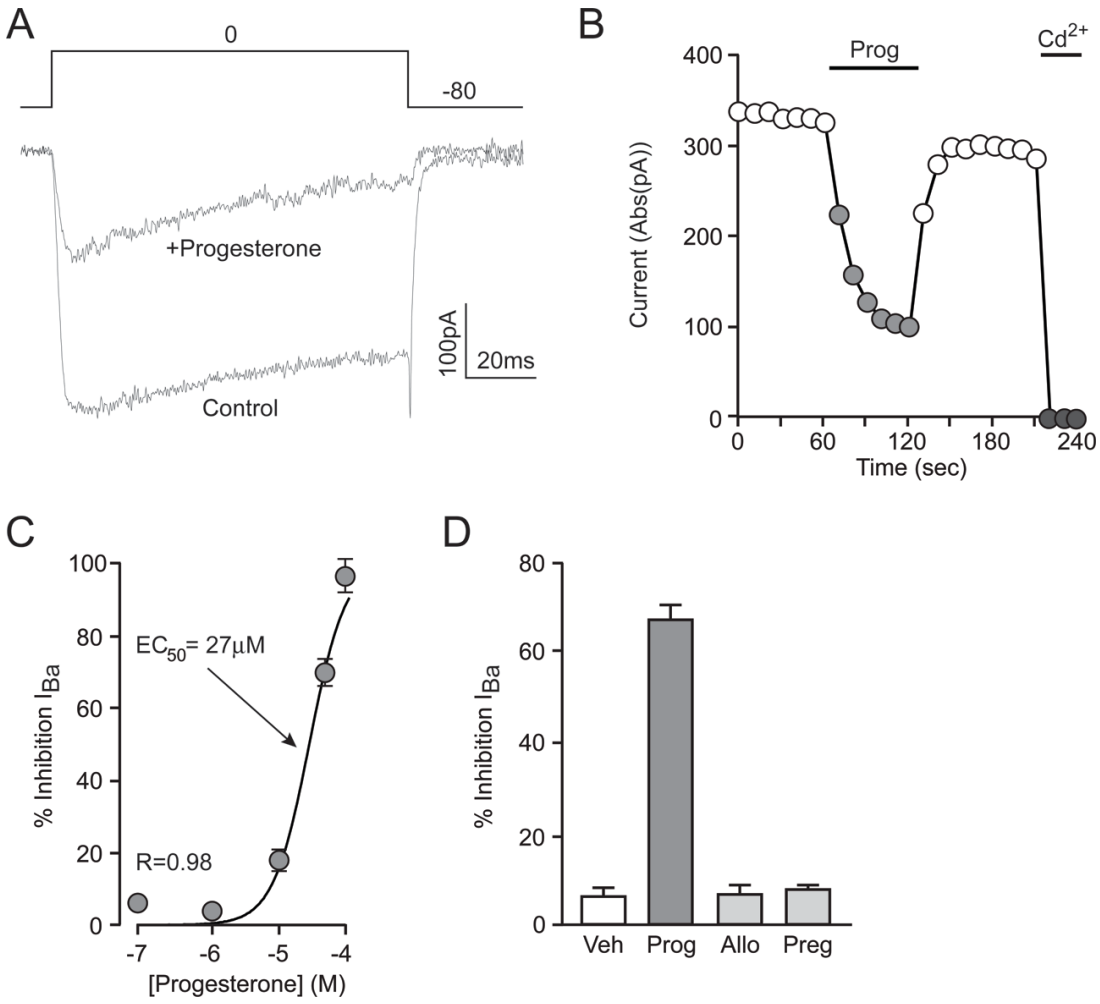

Figure 4. Progesterone inhibits voltage-gated calcium currents. **(**A) Representative traces from a whole-cell voltage clamp recording. Ba^{2+} currents were evoked by a 100 ms step in membrane potential from -80 to 0 mV in the absence or presence of Prog. (B) Time-course of the example

experiment in A, illustrating the rapid onset and washout of Prog-mediated inhibition of calcium channels. 200 μM Cd^{2+} was used to block the whole-cell Ba^{2+} current. (C) Concentration-response curve of Prog-mediated inhibition of I_{Ba}. IC_{50} = 27 μM. ($n \geq 4$ for each point). (D) Summary of results from experiments testing the effects of related compounds on voltage-gated calcium channel activity; Control = 5 ± 2%, Prog = 67 ± 3%, Allo = 7 ± 2%, Preg = 8 ± 1%.

Allopregnanolone and pregnenalone again had no effect (Figure 5A). In order to fully test the specificity of the effect of progesterone on NFAT-dependent transcription, we evaluated not only cholesterol, but also a number of steroid hormones (all at 50 μM) on depolarization-induced NFAT-dependent transcription. Unlike progesterone, cholesterol, estradiol, dihydrotestosterone, and corticosterone were all ineffective in altering depolarization-induced NFAT-dependent transcription (Figure 5B, see discussion). The effect of progesterone on inhibiting activity-dependent gene expression was not exclusive to NFAT. Progesterone also blocked CRE-dependent transcription (Figure 4C,D; IC_{50}=17 μM (data not shown)). Again, there was no effect of the other steroid hormones on CRE-dependent transcription (Figure 5C,D).

Progesterone does not inhibit AMPA or NMDA receptors

Due to the lack of glutamatergic synaptic terminals, the utilization of striatal cultures in these experiments is advantageous as the effects of progesterone on voltage-gated calcium channels can be readily isolated from AMPA and NMDA receptors. The next series of experiments examined the impact of progesterone on glutamate receptors. Using calcium imaging, we found that a 30 second bath

application of glutamate (3 μM) caused a rapid and transient rise in intracellular calcium (Figure 6A). Similar to the 20K depolarization trials, each experiment consisted of three

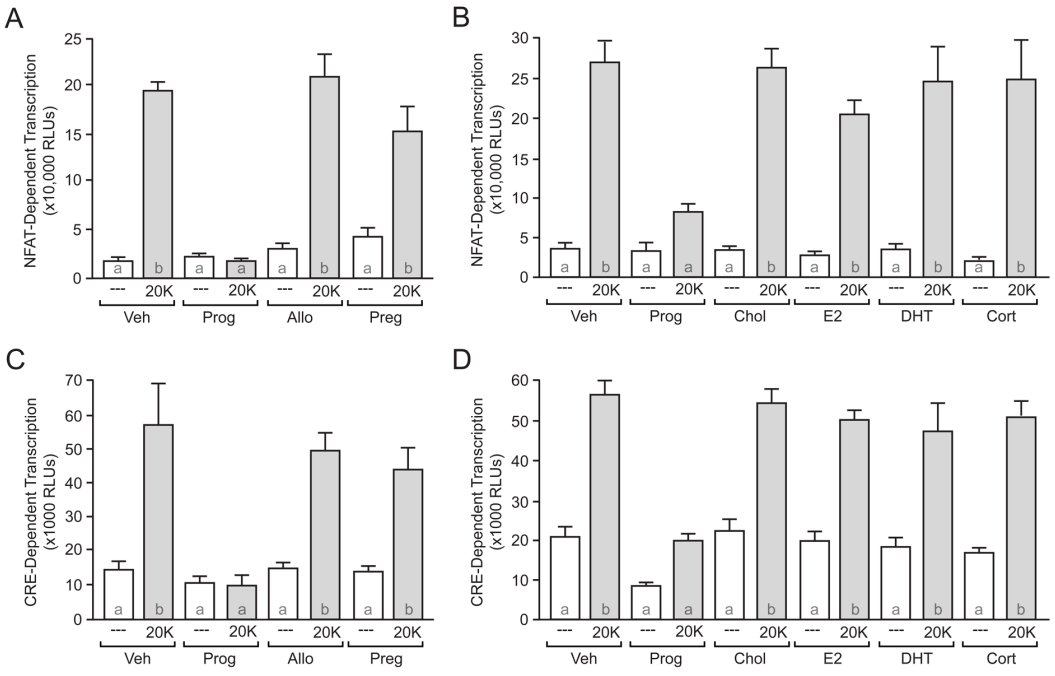

Figure 5. Depolarization-induced calcium signaling is abolished by progesterone. (A-D) Luciferase assay data measuring NFAT- and CRE-dependent transcription. (A,C) 20K produced a significant increase in NFAT- ($F = 20.82$; $t = 6.72$; $p < 0.05$) and CRE- ($F = 31.54$, $t = 7.51$; $p < 0.05$) dependent transcription in the presence of vehicle (Veh). (A-D) These effects were blocked by Prog (50 μM). Preg, Allo, cholesterol (Chol), estradiol (E2) dihydrotestosterone (DHT), or corticosterone (Cort) (all applied at 50 μM) had no effect on 20K-induced gene expression. Letters in bars represent statistically similar groups as analyzed by a one-way ANOVA with Bonferroni post-hoc analysis.

glutamate-evoked peaks, separated by approximately 15 minutes. To verify that this brief glutamate stimulus was not impacting the activity of L-type calcium channels, nifedipine was shown not to affect calcium signals (Figure 6B,F). In comparison, the AMPAR antagonist CNQX (20 μM) attenuated the glutamate-mediated increase in intracellular calcium by 66.7 ± 3 % (Fig 5C,F). Furthermore, the NMDAR antagonist AP5 (25 μM) reduced the glutamate-mediated increase in intracellular calcium by 55.1 ± 3 % (Figure 6D,F). Application of both CNQX and AP5 resulted in a decrease of the calcium signal by 73.4 ± 2 % (data not shown). The residual increase in intracellular calcium following treatment with both CNQX and AP5 is consistent with activation of metabotropic glutamate receptors (Zirpel et al., 1995b). Furthermore, the sub-additive effects of CNQX and AP5 are consistent with traditional AMPA receptor activation leading to stimulation of NMDA receptors. To determine whether progesterone inhibits glutamate-induced calcium influx, glutamate was applied in the presence of 50 μM progesterone. Progesterone was found to have no effect on the glutamate-induced increase in intracellular calcium (Figure 6E,F).

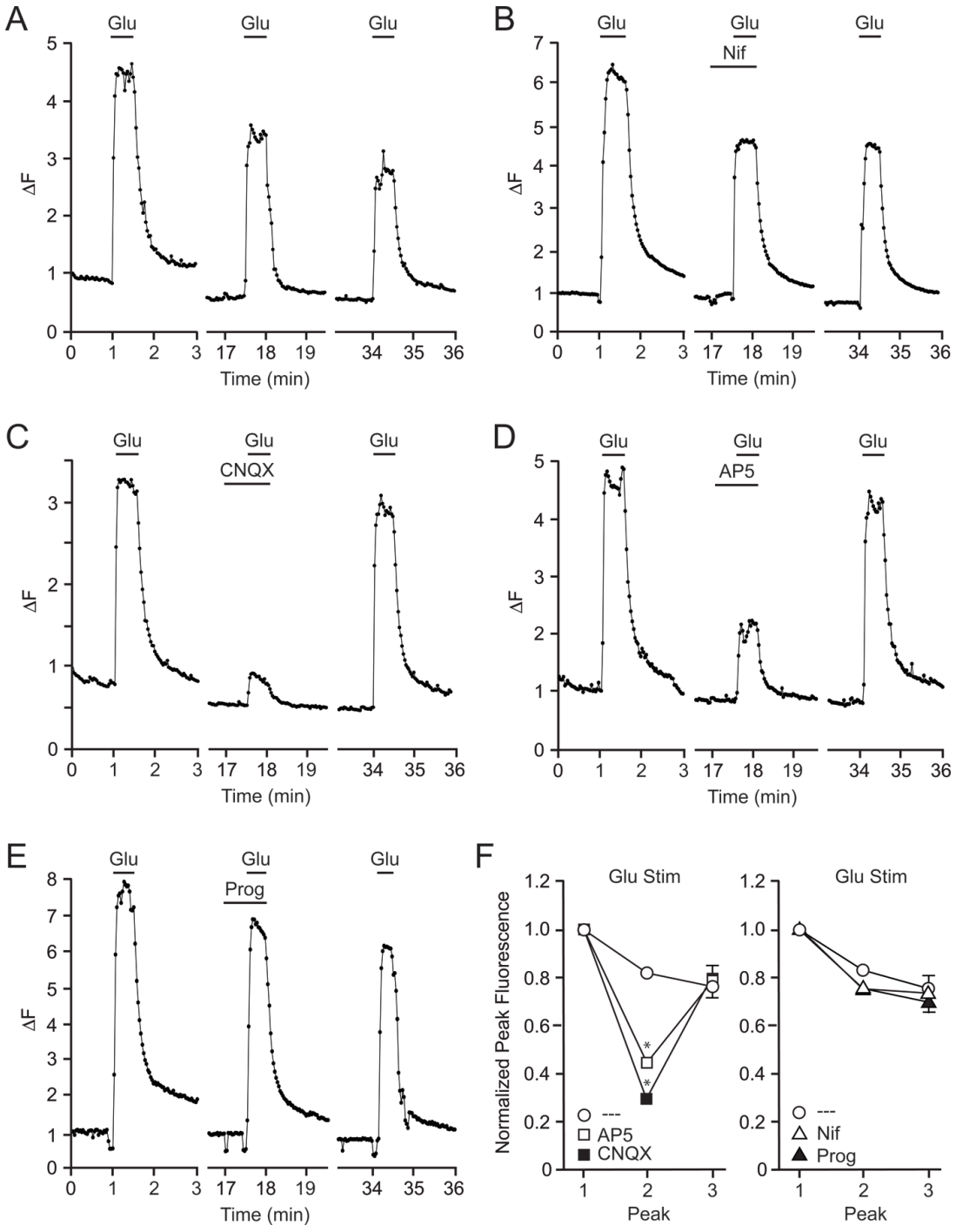

Figure 6. Progesterone does not block glutamate-mediated increases in intracellular calcium. A-E, Example plots of calcium imaging data taken from cultured striatal neurons. (A) Application of 3 μM glutamate (Glu) evoked a reproducible increase in intracellular calcium. (B) The rise in intracellular

calcium following brief application of Glu was not sufficient to activate L-type calcium channels. (C and D) Glutamate-induced increases in intracellular calcium were attenuated following application of either CNQX (20 μM) or AP5 (25 μM). (E) 50 μM Prog did not affect the calcium signal induced by Glu. (F) Data summary illustrating the effects of CNQX ($t = 10.01$; $p < 0.05$) and AP5 ($t = 7.31$; $p < 0.05$) versus Nif ($t = 1.24$; $p > 0.05$) Prog ($t = 0.89$; $p > 0.05$) on Glu-induced increases in intracellular calcium.

These results strongly suggested that progesterone did not affect AMPA or NMDA receptors. To directly test this hypothesis, their specific receptor agonists were applied to individual neurons via a picospritzer during whole-cell voltage clamp experiments. A 200 ms application of AMPA (100 μM) elicited a rapidly inactivating inward current (Figure 7A). Surprisingly, in the presence of progesterone, the amplitude of the AMPA-induced current *increased* by 31 ± 5% (Figure 7C). This effect of progesterone was readily reversible (data not shown). When NMDA (100 μM) was applied in a similar manner, a smaller but more slowly inactivating inward current was observed (Figure 7B). There was no change in the size of the NMDA-mediated current in the presence of progesterone (Figure 7C). These data suggest that the neuroprotective effects of progesterone are not due to a direct inhibition of ionotropic glutamate receptors, but rather highlight the importance of progesterone inhibition of voltage-gated calcium channels.

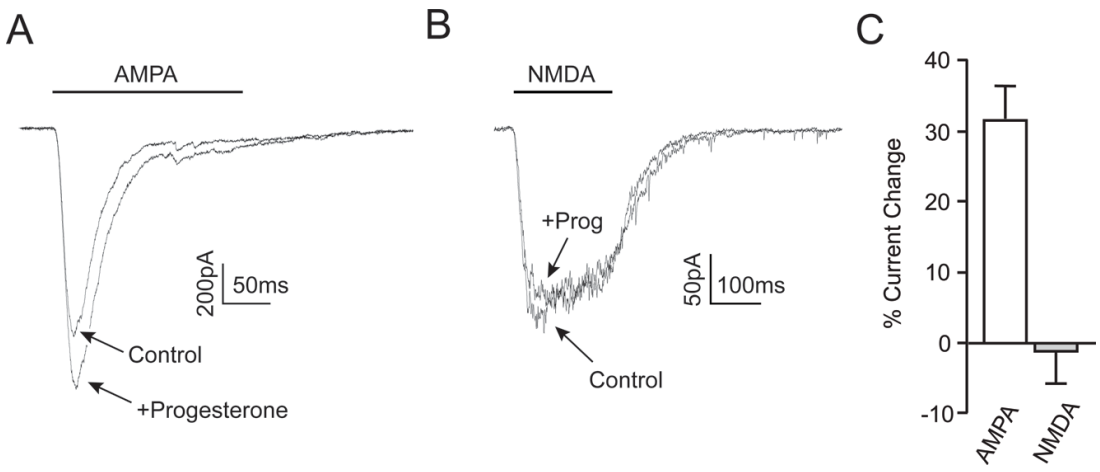

Figure 7. Progesterone does not inhibit ionotropic glutamate receptor signaling. (A and B) Representative traces of whole-cell voltage clamp recordings during a 200 ms picospritzer application of AMPA (100 μM; A) or NMDA (100 μM; B) in the presence or absence of Prog. Progesterone application increased AMPA-mediated currents while having no effect on NMDA-mediated currents. (C) Bar graph summarizing the change in AMPA- and NMDA-mediated peak current size, AMPA = 31 ± 5% (n = 6), NMDA = -1 ± 8% (n = 6).

Discussion

Therapeutic treatment with progesterone following traumatic brain injury has been a safe and useful means of reducing neuronal damage and mortality resulting from brain trauma in early phase clinical trials (Wright et al., 2007; Xiao et al., 2008). Due to its success, progesterone has entered phase III clinical trials despite little being known about the mechanism of its neuroprotective effects. This study intended to provide a putative framework by which progesterone is neuroprotective through analysis of the effects of progesterone on calcium signaling. In terms of neuroprotection, progesterone blocks depolarization-induced cell death. Additionally, progesterone inhibits voltage-gated calcium channels. Through inhibition of L-type calcium channels, progesterone inhibits depolarization-induced CREB and NFAT mediated transcription. All of these effects are steroid specific. The actions of progesterone occur at the neuronal surface, are rapid and reversible, and do not appear to be receptor mediated. The lack of influence on the primary effects of glutamate signaling, specifically glutamate-induced calcium influx and AMPA and NMDA receptor-mediated currents indicates that the location of progesterone-mediated neuroprotection occurs subsequent to glutamate receptor activation. Collectively, these data suggest a progesterone-sensitive pathway for excitotoxicity that progesterone is neuroprotective against (Figure 8).

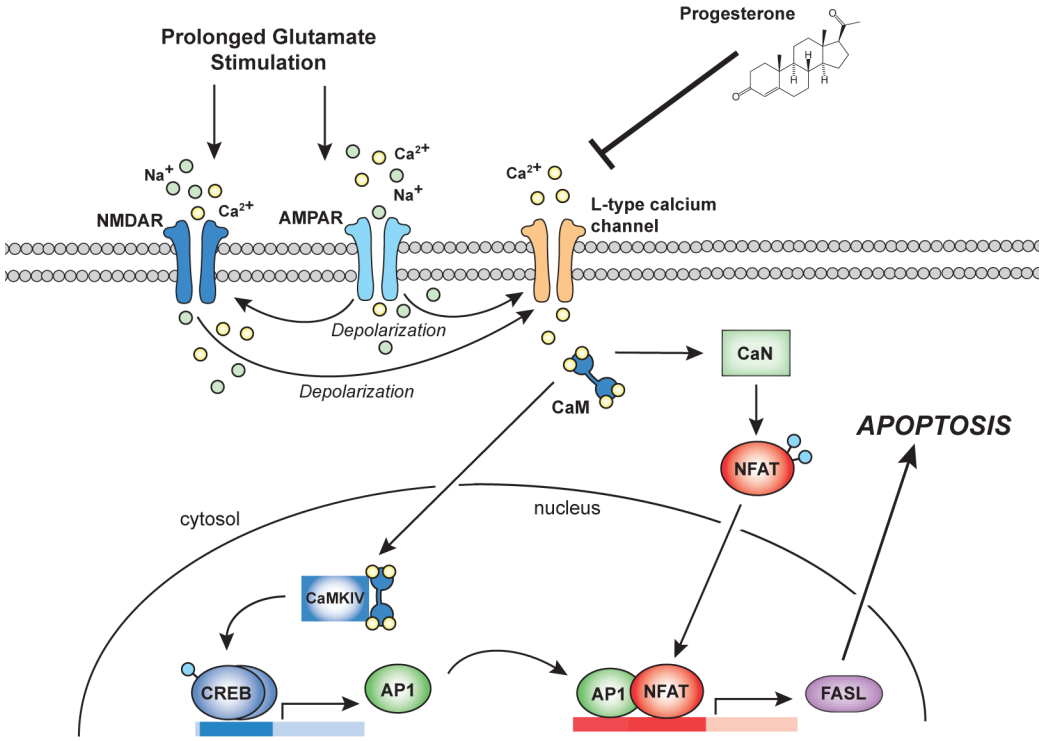

Figure 8. An excitotoxic pathway that progesterone protects against. In this pathway, glutamate stimulation triggers an influx of sodium and calcium ions through AMPARs. Subsequent depolarization leads to activation of NMDARs and L-type calcium channels. Additional influx of sodium and calcium ions through NMDARs contributes to further depolarization and activation of L-type calcium channels. Calcium influx through L-type calcium channels, following prolonged glutamate stimulation, results in calcium overload and eventual neuron death through the activation of activity-dependent transcription factors. This includes the mechanism by which NFAT and CREB activation collectively lead to the expression of FASL and subsequent apoptosis. Progesterone blocks L-type calcium channels and consequently inhibits death mechanisms such as the one depicted here.

The finding that progesterone did not inhibit glutamate signaling initially seemed surprising given the idea that glutamate plays a critical role in the neuron death following brain injury via calcium-mediated mechanisms. Fortunately we were able to isolate the effects of progesterone across different routes of calcium entry. Progesterone-mediated inhibition of voltage-gated calcium channels provides a therapeutic mechanism of action; consistent with previous findings that neuronal death depends on delayed glutamate-dependent activation of L-type calcium channels (Miyazaki et al., 1999; Vallazza-Deschamps et al., 2005; Sribnick et al., 2009). Of critical therapeutic value, the delay in L-type calcium channel signaling following brain injury supports the data that progesterone can be an effective agent in protecting neurons even if administered several hours after injury (Roof et al., 1996; Gibson et al., 2008).

Progesterone attenuation of calcium influx during periods of excessive activity can contribute to neuroprotection via multiple mechanisms. One mechanism is the inhibition of activity-dependent death mechanisms. This would include the inhibition of NFAT- and FASL-dependent apoptosis (Jayanthi et al., 2005; Luoma and Zirpel, 2008). Interestingly, NFAT has also been shown to be involved in the initiation of neuro-inflammation (Sama et al., 2008; Furman et al., 2010), and thus progesterone may be neuroprotective via inhibition of this pathway as well. Interestingly, progesterone-mediated inhibition of CRE-dependent transcription would appear to be counterproductive, as CREB regulates a number of pro-survival genes. However, concurrent blockade of death mechanisms by progesterone would

most likely reduce the need for pro-survival gene expression. Additionally, activation of pathways that result in CREB phosphorylation and CREB activation itself have been implicated in the initiation of apoptosis (Jimenez et al., 1997; Saeki et al., 1999; Barlow et al., 2006).

In addition to intracellular receptors, recent studies have identified membrane associated progestin receptors (Thomas et al., 2004; Sleiter et al., 2009). That said, our findings suggest that these receptors are not responsible for these actions of the hormone. First, the concentrations required for progesterone to exert its neuroprotective effects are beyond that necessary for the activation of progestin receptors. Second, cell dialysis with progesterone had no effect on progesterone-mediated inhibition of voltage-gated calcium channels. Third, in studies that examine the nontraditional actions of progestins via membrane-localized receptors, pregnenalone and allopregnanolone are effective (Ffrench-Mullen et al., 1994; Kokate et al., 1994). Fourth, the fact that progesterone could completely block voltage-gated calcium channels with both rapid onset and offset kinetics further support a unique mode of action. Finally, progesterone has anesthetic effects at micromolar concentrations in progesterone-receptor knock-out mice indicating a non-receptor mediated progesterone effect at therapeutic concentrations (Reddy and Apanites, 2005). While the exact means by which progesterone is able to act at the membrane to inhibit calcium channels remains unknown, the receptor-independent nature of progesterone action provides a therapeutic advantage, as compared for example, to the neuroprotective effects of estradiol, which utilize specific estrogen

receptors (hence will require the expression of receptor to be protective), display sex differences, and often exhibit complex concentration-response relationships (Grove-Strawser et al.; Boulware et al., 2005; Miller et al., 2005; Lebesgue et al., 2009; Mermelstein, 2009; Watson et al., 2009; Lebesgue et al., 2010).

Gonadal synthesis alone is not sufficient for progesterone to reach therapeutic concentrations in the brain. That said, progesterone is also synthesized directly within the nervous system (Sinchak et al., 2003; Schumacher et al., 2004; Micevych et al., 2007). Thus, it is possible that locally synthesized neuroprogesterone could affect cell functioning in ways outlined within this study. Possibly, locally synthesized neuroprogesterone could explain why some brain areas are less susceptible to damage than others (Schmidt-Kastner and Freund, 1991; Candelario-Jalil et al., 2001; Wang and Michaelis, 2010). Future research will need to determine whether brain regions exhibiting neuroprogesterone synthesis are more resistant to neurological insult.

In summary, the data presented here offer a thorough analysis of the effects of therapeutic concentrations of progesterone on voltage-gated calcium channel signaling. The effects of progesterone on voltage-gated calcium channels were determined to be rapid and efficient, consequently having a significant impact on neuronal signaling cascades. These previously undefined effects provide insight into mechanisms that may underlie the neuroprotective effects of progesterone.

Chapter Four

Concluding Statements

A Common Neuroprotective Strategy: Modulation of Calcium Signaling

The studies in this dissertation have demonstrated that modification of calcium signaling is a common strategy for neuroprotection in both deafferented auditory neurons and in the mechanism for neuroprotective effects of progesterone. Here, I have characterized a calcium-mediated pathway by which deafferented auditory neurons die. As a result, we know that inhibiting calcium-dependent events such as NFAT activation is a putative neuroprotective strategy. Also presented here is the profound inhibitory effect of progesterone on voltage-gated calcium channel signaling. Specifically, these studies show that progesterone is able to both significantly inhibit calcium flux through L-type calcium channels and consequently block the downstream effects of calcium influx; thereby exerting its neuroprotective effects.

NFAT Activation in Brain Injury and Stroke

Since the activation of intracellular calcium signaling occurs in both the death pathway for deafferented sensory neurons and in injured neurons, the activation of NFAT may also be a shared downstream target. In the case of deafferented sensory neurons, I found that inhibition of NFAT activation is neuroprotective. Given that progesterone is neuroprotective against excitotoxic neuron death and that it can completely block NFAT activation by inhibiting the calcium signal that triggers its activation, it suggests that one way by which injury-induced excitotoxicity leads to neuron death is through the initiation of NFAT-dependent apoptosis. Thus, it would

be interesting to determine if the NFAT inhibitor, 11R-VIVIT, has neuroprotective effects in models of excitotoxicity, brain injury, or stroke injury.

In support of NFAT playing a role in brain injury is evidence of calcineurin-dependent death of motor neurons following spinal cord ischemia (Sato et al., 2003). Notably, in experimental traumatic brain injury models inhibitors of calcineurin reduce neuronal damage (Scheff and Sullivan, 1999; Sullivan et al., 2000b; Sullivan et al., 2000a). This finding is relevant because NFAT depends on calcineurin for its dephosphorylation and subsequent activation. In addition, both NFAT activation and FASL expression are increased in neurons following middle cerebral artery occlusion (MCAO), a model for brain ischemia (Shioda et al., 2007). Further, there is evidence of increased FASL expression following impact injury in rodents (Beer et al., 2000). Consistent with these data are studies by others that link calcineurin activation to increased FASL expression. Specifically, MCAO induced calcinuerin-dependent FASL expression in rat neuroblastoma cells (Herr et al., 1999; Martin-Villalba et al., 1999). Collectively, these data strongly suggest that NFAT plays a role in injury-induced death of neurons by way of inducing FASL expression. Importantly, this is consistent with what I found in the deafferented auditory neurons.

Progesterone in Activity Deprived Sensory Neurons

Since there are many similarities between deafferentation-induced and brain injury-induced neuronal death, the possibility of progesterone being neuroprotective in activity deprived sensory neurons should be considered. This rationale is based on

the following findings: 1) calcium influx is essential for deafferentation-induced death of auditory neurons, 2) deafferentation-induced apoptosis depends upon the activation of NFAT and 3) progesterone is capable of blocking calcium-mediated NFAT activation. It remains to be determined if deafferentation and excitotoxicity mediate calcium influx via similar mechanisms. In other words, does deafferentation induced excitotoxicity result from an initial ion-flux through AMPA receptors followed by secondary activation of L-type calcium channels? Since deafferentation induced death has been shown to be dependent on AMPAR activation, we could reconcile this by determining if L-type calcium channel blockers are able to rescue neurons from deafferentation-induced death, and also if they block NFAT activation following deafferentation. If so, it is likely that progesterone will have neuroprotective effects in deafferented sensory neurons because of its potent inhibitory effect on both L-type calcium channels and the downstream effects of their activation.

In a number of ways, deafferentation can be considered an injury. In humans, deafferentation of the primary auditory neurons can be due to cochlear hair cell injury or damage from a variety of insults including high intensity noise, head injury, or the use of certain antibiotics. In addition, the widely accepted experimental model for deafferentation of primary auditory neurons is the removal of the entire cochlea by aspiration, which can also be considered an injury since it is actively induced rather than a developmental abnormality. This may explain the similarities in death pathway

characteristics between deafferentation and what is traditionally thought of as brain injury.

Glutamate-Induced Excitotoxicity: Alternative Neuroprotective Effects of Progesterone

Although excessive accumulation of calcium is the predominant mediator of excitotoxic neuron death, signaling cascades triggered by other ions can also contribute to excitotoxicity. For example, inhibition of the flux of chloride-ions through gamma-aminobutyric acid receptors (GABARs) is neuroprotective following application of glutamate (Babot et al., 2005). Furthermore, the removal of extracellular sodium ions or, analogously, blockade of sodium influx eliminates toxic neuronal swelling and reduces death in some models of excitoxicity (Rothman, 1985; Huang et al., 1997; Luo et al., 2004). Similarly, the blockade of potassium currents is neuroprotective against excitotoxicity or ischemia (Huang et al., 2001; Zaks-Makhina et al., 2004). Interestingly, our lab has preliminary data indicating that progesterone significantly reduces the flux of chloride ions through gamma-aminobutyric acid receptors (GABARs) and both potassium and sodium ions through their respective voltage-gated ion channels. Therefore, the neuroprotective effects of progesterone may not be limited to inhibition of calcium influx, but rather extend beyond interactions with calcium signaling. In order to fully understand the neuroprotective effects of molecules like progesterone, future investigations should consider mechanisms that extend beyond modulation of calcium signaling.

Progesterone as a Therapy for Neurodegenerative Disease

Since we have determined that the neuroprotective effects of progesterone are in part routed through the ability of progesterone to block excitotoxicity mediated by the activation of voltage-gated calcium channels, we may now be able to find additional uses for progesterone as a neuroprotective treatment in neurodegenerative disease. Remarkably, the pathophysiology of a variety of neurodegenerative diseases and disorders such Epilepsy, Amyotrophic Lateral Sclerosis (ALS), and Parkinson's disease includes excessive glutamate release, dysregulation of intracellular signaling, perturbed calcium homeostasis, and excitotoxic death of neurons (Caudle and Zhang, 2009; Grosskreutz et al., 2010; Lau and Tymianski, 2010).

Protecting neurons from excitotoxic death with progesterone treatment may slow the progression and improve the outcome of these diseases. For example, hippocampal neurons are particularly sensitive to excitotoxic death resulting from epileptic seizures (Bengzon et al., 1997). In fact, studies have linked voltage-gated calcium channel activity with seizure-induction and subsequent excitotoxicity (Czuczwar et al., 1990; Otoom and Hasan, 2006; Weiergraber et al., 2007). Thus, progesterone may be capable of reducing neuron death from seizure-induced excitotoxicity by inhibiting calcium overload. Additionally, it may inhibit the occurrence of seizures by reducing the overall excitability of the neurons because of its added ability to inhibit voltage-gated sodium channels.

Recent studies have revealed that treatment with dihydropyridines, L-type calcium channel blockers, reduces the risk of developing Parkinson's disease and is a

potential neuroprotective therapy for patients with the disease (Ritz et al.; Pfeiffer, 2010). In our study, we found that either progesterone or the dihydropyridine nifedepine was equally effective at blocking L-type calcium channel mediated neuron death, suggesting that progesterone may have neuroprotective effects for Parkinson's disease patients. In Alzheimer's disease, disruption of calcium homeostasis has been associated with the pathological hallmarks of the disease (Mattson and Chan, 2001). It is thought that dysregulation of calcium homeostasis in these diseased neurons renders them susceptible to excitotoxicity and apoptosis. Interestingly, evidence has shown increased neuronal expression of L-type calcium channels in patients with Alzheimer's disease, which is thought to contribute to neuron death (Coon et al., 1999). Again, progesterone may be a useful therapeutic strategy since it has a profound inhibitory effect on L-type calcium channels.

Closing Statements

In summary, I have delineated molecular mechanisms by which both deafferentation-induced neuronal death, and progesterone-mediated neuroprotection occur. Though seemingly distinct physiological processes, the study of these neuronal processes have illuminated common mechanisms through which neuronal death (and protection from that death) may occur. Specifically, I have found that secondary mechanisms of calcium entry and NFAT-dependent transcription play essential roles in both of these processes, suggesting that the coordinated activity of downstream transcription and translation via calcium signaling represents a fundamental

mechanism for balancing and modulating neuronal survival and death. These results suggest common molecular targets for interventional therapy across a variety of neurodegenerative diseases and injury-related insults.

References

Aramburu J, Yaffe MB, Lopez-Rodriguez C, Cantley LC, Hogan PG, Rao A (1999) Affinity-driven peptide selection of an NFAT inhibitor more selective than cyclosporin A. Science 285:2129-2133.

Arundine M, Tymianski M (2004) Molecular mechanisms of glutamate-dependent neurodegeneration in ischemia and traumatic brain injury. Cell Mol Life Sci 61:657-668.

Atif F, Sayeed I, Ishrat T, Stein DG (2009) Progesterone with vitamin D affords better neuroprotection against excitotoxicity in cultured cortical neurons than progesterone alone. Molecular medicine (Cambridge, Mass) 15:328-336.

Babot Z, Cristofol R, Sunol C (2005) Excitotoxic death induced by released glutamate in depolarized primary cultures of mouse cerebellar granule cells is dependent on GABAA receptors and niflumic acid-sensitive chloride channels. Eur J Neurosci 21:103-112.

Bargas J, Howe A, Eberwine J, Cao Y, Surmeier DJ (1994) Cellular and molecular characterization of Ca2+ currents in acutely isolated, adult rat neostriatal neurons. J Neurosci 14:6667-6686.

Barlow CA, Shukla A, Mossman BT, Lounsbury KM (2006) Oxidant-mediated cAMP response element binding protein activation: calcium regulation and role in apoptosis of lung epithelial cells. Am J Respir Cell Mol Biol 34:7-14.

Beer R, Franz G, Schopf M, Reindl M, Zelger B, Schmutzhard E, Poewe W, Kampfl A (2000) Expression of Fas and Fas ligand after experimental traumatic brain injury in the rat. J Cereb Blood Flow Metab 20:669-677.

Bender C, Rassetto M, Olmos JS, Olmos SD, Lorenzo A (2009) Involvement of AMPA/kainate-excitotoxicity in MK801-induced neuronal death in the retrosplenial cortex. Neuroscience.

Bengzon J, Kokaia Z, Elmer E, Nanobashvili A, Kokaia M, Lindvall O (1997) Apoptosis and proliferation of dentate gyrus neurons after single and intermittent limbic seizures. Proc Natl Acad Sci U S A 94:10432-10437.

Bielefeldt K, Waite L, Abboud FM, Conklin JL (1996) Nongenomic effects of progesterone on human intestinal smooth muscle cells. Am J Physiol 271:G370-376.

Born DE, Rubel EW (1985) Afferent influences on brain stem auditory nuclei of the chicken: neuron number and size following cochlea removal. J Comp Neurol 231:435-445.

Boulware MI, Weick JP, Becklund BR, Kuo SP, Groth RD, Mermelstein PG (2005) Estradiol activates group I and II metabotropic glutamate receptor signaling, leading to opposing influences on cAMP response element-binding protein. J Neurosci 25:5066-5078.

Bradley KC, Groth RD, Mermelstein PG (2005) Immunolocalization of NFATc4 in the adult mouse brain. J Neurosci Res 82:762-770.

Candelario-Jalil E, Al-Dalain SM, Castillo R, Martinez G, Fernandez OS (2001) Selective vulnerability to kainate-induced oxidative damage in different rat brain regions. J Appl Toxicol 21:403-407.

Catsicas M, Pequignot Y, Clarke PG (1992) Rapid onset of neuronal death induced by blockade of either axoplasmic transport or action potentials in afferent fibers during brain development. J Neurosci 12:4642-4650.

Caudle WM, Zhang J (2009) Glutamate, excitotoxicity, and programmed cell death in Parkinson disease. Exp Neurol 220:230-233.

Choi DW (1985) Glutamate neurotoxicity in cortical cell culture is calcium dependent. Neuroscience Letters 58:293-297.

Coon AL, Wallace DR, Mactutus CF, Booze RM (1999) L-type calcium channels in the hippocampus and cerebellum of Alzheimer's disease brain tissue. Neurobiol Aging 20:597-603.

Crabtree GR, Olson EN (2002) NFAT signaling: choreographing the social lives of cells. Cell 109 Suppl:S67-79.

Czuczwar SJ, Malek U, Kleinrok Z (1990) Influence of calcium channel inhibitors upon the anticonvulsant efficacy of common antiepileptics against pentylenetetrazol-induced convulsions in mice. Neuropharmacology 29:943-948.

Deisseroth K, Mermelstein PG, Xia H, Tsien RW (2003) Signaling from synapse to nucleus: the logic behind the mechanisms. Curr Opin Neurobiol 13:354-365.

Dolmetsch RE, Lewis RS, Goodnow CC, Healy JI (1997) Differential activation of transcription factors induced by Ca2+ response amplitude and duration. Nature 386:855-858.

Ffrench-Mullen JM, Danks P, Spence KT (1994) Neurosteroids modulate calcium currents in hippocampal CA1 neurons via a pertussis toxin-sensitive G-protein-coupled mechanism. J Neurosci 14:1963-1977.

Flockhart RJ, Diffey BL, Farr PM, Lloyd J, Reynolds NJ (2008) NFAT regulates induction of COX-2 and apoptosis of keratinocytes in response to ultraviolet radiation exposure. Faseb J 22:4218-4227.

Franks KM, Sejnowski TJ (2002) Complexity of calcium signaling in synaptic spines. Bioessays 24:1130-1144.

Furman JL, Artiushin IA, Norris CM (2010) Disparate effects of serum on basal and evoked NFAT activity in primary astrocyte cultures. Neurosci Lett 469:365-369.

Furuke K, Shiraishi M, Mostowski HS, Bloom ET (1999) Fas ligand induction in human NK cells is regulated by redox through a calcineurin-nuclear factors of activated T cell-dependent pathway. J Immunol 162:1988-1993.

Garden GA, Redeker-DeWulf V, Rubel EW (1995) Afferent influences on brainstem auditory nuclei of the chicken: regulation of transcriptional activity following cochlea removal. J Comp Neurol 359:412-423.

Gibson CL, Gray LJ, Bath PM, Murphy SP (2008) Progesterone for the treatment of experimental brain injury; a systematic review. Brain 131:318-328.

Globus MY, Alonso O, Dietrich WD, Busto R, Ginsberg MD (1995) Glutamate release and free radical production following brain injury: effects of posttraumatic hypothermia. J Neurochem 65:1704-1711.

Goss CW, Hoffman SW, Stein DG (2003) Behavioral effects and anatomic correlates after brain injury: a progesterone dose-response study. Pharmacol Biochem Behav 76:231-242.

Graef IA, Mermelstein PG, Stankunas K, Neilson JR, Deisseroth K, Tsien RW, Crabtree GR (1999) L-type calcium channels and GSK-3 regulate the activity of NF-ATc4 in hippocampal neurons. Nature 401:703-708.

Grosskreutz J, Van Den Bosch L, Keller BU (2010) Calcium dysregulation in amyotrophic lateral sclerosis. Cell Calcium 47:165-174.

Groth RD, Mermelstein PG (2003) Brain-derived neurotrophic factor activation of NFAT (nuclear factor of activated T-cells)-dependent transcription: a role for the transcription factor NFATc4 in neurotrophin-mediated gene expression. J Neurosci 23:8125-8134.

Groth RD, Weick JP, Bradley KC, Luoma JI, Aravamudan B, Klug JR, Thomas MJ, Mermelstein PG (2008) D1 dopamine receptor activation of NFAT-mediated striatal gene expression. Eur J Neurosci 27:31-42.

Grove-Strawser D, Boulware MI, Mermelstein PG Membrane estrogen receptors activate the metabotropic glutamate receptors mGluR5 and mGluR3 to bidirectionally regulate CREB phosphorylation in female rat striatal neurons. Neuroscience 170:1045-1055.

Guan YG, Wang TH, Ni W, Li L, Lu YC, Gao ZY (2005) [Distribution of Fas and FasL in the central nervous system of adult rhesus]. Sichuan Da Xue Xue Bao Yi Xue Ban 36:322-324.

Gupta RC, Khandelwal RL, Sulakhe PV (1985) Isolation and characterization of calcineurin from bovine brain. Can J Physiol Pharmacol 63:1000-1006.

Harris JA, Hardie NA, Bermingham-McDonogh O, Rubel EW (2005) Gene expression differences over a critical period of afferent-dependent neuron survival in the mouse auditory brainstem. J Comp Neurol 493:460-474.

Hashisaki GT, Rubel EW (1989) Effects of unilateral cochlea removal on anteroventral cochlear nucleus neurons in developing gerbils. J Comp Neurol 283:5-73.

Hernandez-Ochoa EO, Contreras M, Cseresnyes Z, Schneider MF (2006) Ca(2+) signal summation and NFATc1 nuclear translocation in sympathetic ganglion neurons during repetitive action potentials. Cell Calcium.

Herr I, Martin-Villalba A, Kurz E, Roncaioli P, Schenkel J, Cifone MG, Debatin KM (1999) FK506 prevents stroke-induced generation of ceramide and apoptosis signaling. Brain Res 826:210-219.

Ho SN, Thomas DJ, Timmerman LA, Li X, Francke U, Crabtree GR (1995) NFATc3, a lymphoid-specific NFATc family member that is calcium-regulated and exhibits distinct DNA binding specificity. J Biol Chem 270:19898-19907.

Holtz-Heppelmann CJ, Algeciras A, Badley AD, Paya CV (1998) Transcriptional regulation of the human FasL promoter-enhancer region. J Biol Chem 273:4416-4423.

Huang CS, Song JH, Nagata K, Yeh JZ, Narahashi T (1997) Effects of the neuroprotective agent riluzole on the high voltage-activated calcium channels of rat dorsal root ganglion neurons. J Pharmacol Exp Ther 282:1280-1290.

Huang H, Gao TM, Gong L, Zhuang Z, Li X (2001) Potassium channel blocker TEA prevents CA1 hippocampal injury following transient forebrain ischemia in adult rats. Neurosci Lett 305:83-86.

Itoh N, Tsujimoto Y, Nagata S (1993) Effect of bcl-2 on Fas antigen-mediated cell death. J Immunol 151:621-627.

Itoh N, Yonehara S, Ishii A, Yonehara M, Mizushima S, Sameshima M, Hase A, Seto Y, Nagata S (1991) The polypeptide encoded by the cDNA for human cell surface antigen Fas can mediate apoptosis. Cell 66:233-243.

Jain J, McCaffrey PG, Miner Z, Kerppola TK, Lambert JN, Verdine GL, Curran T, Rao A (1993) The T-cell transcription factor NFATp is a substrate for calcineurin and interacts with Fos and Jun. Nature 365:352-355.

Jayanthi S, Deng X, Ladenheim B, McCoy MT, Cluster A, Cai NS, Cadet JL (2005) Calcineurin/NFAT-induced up-regulation of the Fas ligand/Fas death pathway is involved in methamphetamine-induced neuronal apoptosis. Proc Natl Acad Sci U S A 102:868-873.

Jimenez LA, Zanella C, Fung H, Janssen YM, Vacek P, Charland C, Goldberg J, Mossman BT (1997) Role of extracellular signal-regulated protein kinases in apoptosis by asbestos and H2O2. Am J Physiol 273:L1029-1035.

Kim MS, Usachev YM (2009) Mitochondrial Ca2+ cycling facilitates activation of the transcription factor NFAT in sensory neurons. J Neurosci 29:12101-12114.

Kinjo K, Sandoval S, Sakamoto KM, Shankar DB (2005) The role of CREB as a proto-oncogene in hematopoiesis. Cell Cycle 4:1134-1135.

Klee CB, Crouch TH, Krinks MH (1979) Calcineurin: a calcium- and calmodulin-binding protein of the nervous system. Proc Natl Acad Sci U S A 76:6270-6273.

Kokate TG, Svensson BE, Rogawski MA (1994) Anticonvulsant activity of neurosteroids: correlation with gamma-aminobutyric acid-evoked chloride current potentiation. J Pharmacol Exp Ther 270:1223-1229.

Kondo E, Harashima A, Takabatake T, Takahashi H, Matsuo Y, Yoshino T, Orita K, Akagi T (2003) NF-ATc2 induces apoptosis in Burkitt's lymphoma cells through signaling via the B cell antigen receptor. Eur J Immunol 33:1-11.

Latinis KM, Norian LA, Eliason SL, Koretzky GA (1997) Two NFAT transcription factor binding sites participate in the regulation of CD95 (Fas) ligand expression in activated human T cells. J Biol Chem 272:31427-31434.

Lau A, Tymianski M (2010) Glutamate receptors, neurotoxicity and neurodegeneration. Pflugers Arch 460:525-542.

Lebesgue D, Chevaleyre V, Zukin RS, Etgen AM (2009) Estradiol rescues neurons from global ischemia-induced cell death: multiple cellular pathways of neuroprotection. Steroids 74:555-561.

Lebesgue D, Traub M, De Butte-Smith M, Chen C, Zukin RS, Kelly MJ, Etgen AM (2010) Acute administration of non-classical estrogen receptor agonists attenuates ischemia-induced hippocampal neuron loss in middle-aged female rats. PLoS One 5:e8642.

Lipton SA (1986) Blockade of electrical activity promotes the death of mammalian retinal ganglion cells in culture. Proc Natl Acad Sci U S A 83:9774-9778.

Liu J, Farmer JD, Jr., Lane WS, Friedman J, Weissman I, Schreiber SL (1991) Calcineurin is a common target of cyclophilin-cyclosporin A and FKBP-FK506 complexes. Cell 66:807-815.

Livak KJ, Schmittgen TD (2001) Analysis of relative gene expression data using real-time quantitative PCR and the 2(-Delta Delta C(T)) Method. Methods 25:402-408.

Loh C, Shaw KT, Carew J, Viola JP, Luo C, Perrino BA, Rao A (1996) Calcineurin binds the transcription factor NFAT1 and reversibly regulates its activity. J Biol Chem 271:10884-10891.

Lu Y, Harris JA, Rubel EW (2007) Development of spontaneous miniature EPSCs in mouse AVCN neurons during a critical period of afferent-dependent neuron survival. J Neurophysiol 97:635-646.

Luo C, Burgeon E, Carew JA, McCaffrey PG, Badalian TM, Lane WS, Hogan PG, Rao A (1996) Recombinant NFAT1 (NFATp) is regulated by calcineurin in T cells and mediates transcription of several cytokine genes. Mol Cell Biol 16:3955-3966.

Luo X, Baba A, Matsuda T, Romano C (2004) Susceptibilities to and mechanisms of excitotoxic cell death of adult mouse inner retinal neurons in dissociated culture. Invest Ophthalmol Vis Sci 45:4576-4582.

Luoma JI, Zirpel L (2008) Deafferentation-induced activation of NFAT (nuclear factor of activated T-cells) in cochlear nucleus neurons during a developmental critical period: a role for NFATc4-dependent apoptosis in the CNS. J Neurosci 28:3159-3169.

Macian F, Garcia-Rodriguez C, Rao A (2000) Gene expression elicited by NFAT in the presence or absence of cooperative recruitment of Fos and Jun. Embo J 19:4783-4795.

Macian F, Lopez-Rodriguez C, Rao A (2001) Partners in transcription: NFAT and AP-1. Oncogene 20:2476-2489.

Martin-Villalba A, Herr I, Jeremias I, Hahne M, Brandt R, Vogel J, Schenkel J, Herdegen T, Debatin KM (1999) CD95 ligand (Fas-L/APO-1L) and tumor necrosis factor-related apoptosis-inducing ligand mediate ischemia-induced apoptosis in neurons. J Neurosci 19:3809-3817.

Mattson MP, Chan SL (2001) Dysregulation of cellular calcium homeostasis in Alzheimer's disease: bad genes and bad habits. J Mol Neurosci 17:205-224.

Mermelstein PG (2009) Membrane-localised oestrogen receptor alpha and beta influence neuronal activity through activation of metabotropic glutamate receptors. J Neuroendocrinol 21:257-262.

Mermelstein PG, Bito H, Deisseroth K, Tsien RW (2000) Critical dependence of cAMP response element-binding protein phosphorylation on L-type calcium channels supports a selective response to EPSPs in preference to action potentials. J Neurosci 20:266-273.

Micevych PE, Chaban V, Ogi J, Dewing P, Lu JK, Sinchak K (2007) Estradiol stimulates progesterone synthesis in hypothalamic astrocyte cultures. Endocrinology 148:782-789.

Miller NR, Jover T, Cohen HW, Zukin RS, Etgen AM (2005) Estrogen can act via estrogen receptor alpha and beta to protect hippocampal neurons against global ischemia-induced cell death. Endocrinology 146:3070-3079.

Miyazaki H, Tanaka S, Fujii Y, Shimizu K, Nagashima K, Kamibayashi M, Uehara T, Okuma Y, Nomura Y (1999) Neuroprotective effects of a dihydropyridine derivative, 1,4-dihydro-2,6-dimethyl-4-(3-nitrophenyl)-3,5-pyridinedicarbox ylic acid methyl 6-(5-phenyl-3-pyrazolyloxy)hexyl ester (CV-159), on rat ischemic brain injury. Life Sci 64:869-878.

Molkentin JD, Lu JR, Antos CL, Markham B, Richardson J, Robbins J, Grant SR, Olson EN (1998) A calcineurin-dependent transcriptional pathway for cardiac hypertrophy. Cell 93:215-228.

Mostafapour SP, Del Puerto NM, Rubel EW (2002) bcl-2 Overexpression eliminates deprivation-induced cell death of brainstem auditory neurons. J Neurosci 22:4670-4674.

Mostafapour SP, Cochran SL, Del Puerto NM, Rubel EW (2000) Patterns of cell death in mouse anteroventral cochlear nucleus neurons after unilateral cochlea removal. J Comp Neurol 426:561-571.

Noguchi H, Matsushita M, Okitsu T, Moriwaki A, Tomizawa K, Kang S, Li ST, Kobayashi N, Matsumoto S, Tanaka K, Tanaka N, Matsui H (2004) A new cell-permeable peptide allows successful allogeneic islet transplantation in mice. Nat Med 10:305-309.

Northrop JP, Ho SN, Chen L, Thomas DJ, Timmerman LA, Nolan GP, Admon A, Crabtree GR (1994) NF-AT components define a family of transcription factors targeted in T-cell activation. Nature 369:497-502.

Oertel D, Young ED (2004) What's a cerebellar circuit doing in the auditory system? Trends Neurosci 27:104-110.

Otoom S, Hasan Z (2006) Nifedipine inhibits picrotoxin-induced seizure activity: further evidence on the involvement of L-type calcium channel blockers in epilepsy. Fundam Clin Pharmacol 20:115-119.

Ozacmak VH, Sayan H (2009) The effects of 17beta estradiol, 17alpha estradiol and progesterone on oxidative stress biomarkers in ovariectomized female rat brain subjected to global cerebral ischemia. Physiol Res 58:909-912.

Parks TN (1999) Cochlear influences on development of the brainstem auditory system. In: The Biology of Early Influences (Hyson RL, Johnson F, eds), pp 15-34. New York: Academic Press.

Paxinos G, Franklin KBJ (2001) The Mouse Brain in Stereotaxic Coordinates, 2 Edition: Academic Press.

Pfeiffer RF (2010) Parkinson disease: calcium channel blockers and Parkinson disease. Nat Rev Neurol 6:188-189.

Rao A, Luo C, Hogan PG (1997) Transcription factors of the NFAT family: regulation and function. Annu Rev Immunol 15:707-747.

Raoul C, Henderson CE, Pettmann B (1999) Programmed cell death of embryonic motoneurons triggered through the Fas death receptor. J Cell Biol 147:1049-1062.

Raoul C, Estevez AG, Nishimune H, Cleveland DW, deLapeyriere O, Henderson CE, Haase G, Pettmann B (2002) Motoneuron death triggered by a specific pathway downstream of Fas. potentiation by ALS-linked SOD1 mutations. Neuron 35:1067-1083.

Reddy DS, Apanites LA (2005) Anesthetic effects of progesterone are undiminished in progesterone receptor knockout mice. Brain Res 1033:96-101.

Ritz B, Rhodes SL, Qian L, Schernhammer E, Olsen JH, Friis S L-type calcium channel blockers and Parkinson disease in Denmark. Ann Neurol 67:600-606.

Robertson CL, Puskar A, Hoffman GE, Murphy AZ, Saraswati M, Fiskum G (2006) Physiologic progesterone reduces mitochondrial dysfunction and hippocampal cell loss after traumatic brain injury in female rats. Exp Neurol 197:235-243.

Roof RL, Duvdevani R, Heyburn JW, Stein DG (1996) Progesterone rapidly decreases brain edema: treatment delayed up to 24 hours is still effective. Exp Neurol 138:246-251.

Rothman SM (1985) The neurotoxicity of excitatory amino acids is produced by passive chloride influx. J Neurosci 5:1483-1489.

Rubel EW, T.N. Parks, and L. Zirpel (2004) Assembling, connecting and innervating the cochlear nucleus.: op. cit.

Ruff VA, Leach KL (1995) Direct demonstration of NFATp dephosphorylation and nuclear localization in activated HT-2 cells using a specific NFATp polyclonal antibody. J Biol Chem 270:22602-22607.

Saeki K, Yuo A, Suzuki E, Yazaki Y, Takaku F (1999) Aberrant expression of cAMP-response-element-binding protein ('CREB') induces apoptosis. Biochem J 343 Pt 1:249-255.

Sama MA, Mathis DM, Furman JL, Abdul HM, Artiushin IA, Kraner SD, Norris CM (2008) Interleukin-1beta-dependent signaling between astrocytes and neurons depends critically on astrocytic calcineurin/NFAT activity. J Biol Chem 283:21953-21964.

Sato M, Horinouchi T, Sakurai M, Murakami N, Sato S, Kato M (2003) Cyclosporin A reduces delayed motor neuron death after spinal cord ischemia in rabbits. Ann Thorac Surg 75:1294-1299.

Sayeed I, Guo Q, Hoffman SW, Stein DG (2006) Allopregnanolone, a progesterone metabolite, is more effective than progesterone in reducing cortical infarct volume after transient middle cerebral artery occlusion. Annals of emergency medicine 47:381-389.

Schauwecker PE (2010) Neuroprotection by glutamate receptor antagonists against seizure-induced excitotoxic cell death in the aging brain. Exp Neurol 224:207-218.

Scheff SW, Sullivan PG (1999) Cyclosporin A significantly ameliorates cortical damage following experimental traumatic brain injury in rodents. J Neurotrauma 16:783-792.

Schmidt-Kastner R, Freund TF (1991) Selective vulnerability of the hippocampus in brain ischemia. Neuroscience 40:599-636.

Schumacher M, Guennoun R, Robert F, Carelli C, Gago N, Ghoumari A, Gonzalez Deniselle MC, Gonzalez SL, Ibanez C, Labombarda F, Coirini H, Baulieu EE, De Nicola AF (2004) Local synthesis and dual actions of progesterone in the nervous system: neuroprotection and myelination. Growth Horm IGF Res 14 Suppl A:S18-33.

Sheng M, McFadden G, Greenberg ME (1990) Membrane depolarization and calcium induce c-fos transcription via phosphorylation of transcription factor CREB. Neuron 4:571-582.

Shioda N, Han F, Moriguchi S, Fukunaga K (2007) Constitutively active calcineurin mediates delayed neuronal death through Fas-ligand expression via activation of NFAT and FKHR transcriptional activities in mouse brain ischemia. J Neurochem 102:1506-1517.

Simmons PA, Rafols JA, Getchell TV (1981) Ultrastructural changes in olfactory receptor neurons following olfactory nerve section. J Comp Neurol 197:237-257.

Sinchak K, Mills RH, Tao L, LaPolt P, Lu JK, Micevych P (2003) Estrogen induces de novo progesterone synthesis in astrocytes. Dev Neurosci 25:343-348.

Sleiter N, Pang Y, Park C, Horton TH, Dong J, Thomas P, Levine JE (2009) Progesterone receptor A (PRA) and PRB-independent effects of progesterone on gonadotropin-releasing hormone release. Endocrinology 150:3833-3844.

Solum D, Hughes D, Major MS, Parks TN (1997) Prevention of normally occurring and deafferentation-induced neuronal death in chick brainstem auditory neurons by periodic blockade of AMPA/kainate receptors. J Neurosci 17:4744-4751.

Sribnick EA, Del Re AM, Ray SK, Woodward JJ, Banik NL (2009) Estrogen attenuates glutamate-induced cell death by inhibiting Ca2+ influx through L-type voltage-gated Ca2+ channels. Brain Res 1276:159-170.

Srivastava RK, Sasaki CY, Hardwick JM, Longo DL (1999) Bcl-2-mediated drug resistance: inhibition of apoptosis by blocking nuclear factor of activated T lymphocytes (NFAT)-induced Fas ligand transcription. J Exp Med 190:253-265.

Steiner JP, Dawson TM, Fotuhi M, Glatt CE, Snowman AM, Cohen N, Snyder SH (1992) High brain densities of the immunophilin FKBP colocalized with calcineurin. Nature 358:584-587.

Suda T, Nagata S (1994) Purification and characterization of the Fas-ligand that induces apoptosis. J Exp Med 179:873-879.

Sullivan PG, Thompson M, Scheff SW (2000a) Continuous infusion of cyclosporin A postinjury significantly ameliorates cortical damage following traumatic brain injury. Exp Neurol 161:631-637.

Sullivan PG, Rabchevsky AG, Hicks RR, Gibson TR, Fletcher-Turner A, Scheff SW (2000b) Dose-response curve and optimal dosing regimen of cyclosporin A after traumatic brain injury in rats. Neuroscience 101:289-295.

Szydlowska K, Tymianski M (2010) Calcium, ischemia and excitotoxicity. Cell Calcium 47:122-129.

Taha SA, Stryker MP (2005) Molecular substrates of plasticity in the developing visual cortex. Prog Brain Res 147:103-114.

Thomas P, Pang Y, Zhu Y, Detweiler C, Doughty K (2004) Multiple rapid progestin actions and progestin membrane receptor subtypes in fish. Steroids 69:567-573.

Tierney TS, Moore DR (1997) Naturally occurring neuron death during postnatal development of the gerbil ventral cochlear nucleus begins at the onset of hearing. J Comp Neurol 387:421-429.

Tierney TS, Russell FA, Moore DR (1997) Susceptibility of developing cochlear nucleus neurons to deafferentation-induced death abruptly ends just before the onset of hearing. J Comp Neurol 378:295-306.

Trune DR (1982) Influence of neonatal cochlear removal on the development of mouse cochlear nucleus: II. Dendritic morphometry of its neurons. J Comp Neurol 209:425-434.

Tymianski M, Tator CH (1996) Normal and abnormal calcium homeostasis in neurons: a basis for the pathophysiology of traumatic and ischemic central nervous system injury. Neurosurgery 38:1176-1195.

Vallazza-Deschamps G, Fuchs C, Cia D, Tessier LH, Sahel JA, Dreyfus H, Picaud S (2005) Diltiazem-induced neuroprotection in glutamate excitotoxicity and ischemic insult of retinal neurons. Doc Ophthalmol 110:25-35.

Vandromme M, Melton SM, Kerby JD (2008) Progesterone in traumatic brain injury: time to move on to phase III trials. Crit Care 12:153.

Walton MR, Dragunow I (2000) Is CREB a key to neuronal survival? Trends Neurosci 23:48-53.

Wang X, Michaelis EK (2010) Selective neuronal vulnerability to oxidative stress in the brain. Front Aging Neurosci 2:12.

Watson CS, Jeng YJ, Kochukov MY (2009) Nongenomic signaling pathways of estrogen toxicity. Toxicol Sci 115:1-11.

Weick JP, Kuo SP, Mermelstein PG (2005) L-type Calcium Channel Regulation of Neuronal Gene Expression. Cellscience 1.

Weick JP, Groth RD, Isaksen AL, Mermelstein PG (2003) Interactions with PDZ proteins are required for L-type calcium channels to activate cAMP response element-binding protein-dependent gene expression. J Neurosci 23:3446-3456.

Weiergraber M, Henry M, Radhakrishnan K, Hescheler J, Schneider T (2007) Hippocampal seizure resistance and reduced neuronal excitotoxicity in mice lacking the Cav2.3 E/R-type voltage-gated calcium channel. J Neurophysiol 97:3660-3669.

Woischwill C, Karczewski P, Bartsch H, Luther HP, Kott M, Haase H, Morano I (2005) Regulation of the human atrial myosin light chain 1 promoter by Ca2+-calmodulin-dependent signaling pathways. Faseb J 19:503-511.

Wright DW. "Progesterone for the Treatment of Traumatic Brain Injury (ProTECT III)." ClinicalTrials.gov. November 18, 2010. Web. January 14, 2009. http://clinicaltrials.gov/ct2/show/NCT00822900

Wright DW, Kellermann AL, Hertzberg VS, Clark PL, Frankel M, Goldstein FC, Salomone JP, Dent LL, Harris OA, Ander DS, Lowery DW, Patel MM, Denson DD, Gordon AB, Wald MM, Gupta S, Hoffman SW, Stein DG (2007) ProTECT: a randomized clinical trial of progesterone for acute traumatic brain injury. Ann Emerg Med 49:391-402, 402 e391-392.

Xiao G, Wei J, Yan W, Wang W, Lu Z (2008) Improved outcomes from the administration of progesterone for patients with acute severe traumatic brain injury: a randomized controlled trial. Crit Care 12:R61.

Xu J, Kurup P, Zhang Y, Goebel-Goody SM, Wu PH, Hawasli AH, Baum ML, Bibb JA, Lombroso PJ (2009) Extrasynaptic NMDA receptors couple preferentially to excitotoxicity via calpain-mediated cleavage of STEP. J Neurosci 29:9330-9343.

Zaks-Makhina E, Kim Y, Aizenman E, Levitan ES (2004) Novel neuroprotective K+ channel inhibitor identified by high-throughput screening in yeast. Mol Pharmacol 65:214-219.

Zhang YJ, Mei HS, Wang C, Wang YL, Zhang YJ (2005) Involvement of nuclear factor of activated T-cells (NFATc) in calcineurin-mediated ischemic brain damage in vivo. Yao Xue Xue Bao 40:299-305.

Zirpel L, Lachica EA, Lippe WR (1995a) Deafferentation increases the intracellular calcium of cochlear nucleus neurons in the embryonic chick. J Neurophysiol 74:1355-1357.

Zirpel L, Lachica EA, Rubel EW (1995b) Activation of a metabotropic glutamate receptor increases intracellular calcium concentrations in neurons of the avian cochlear nucleus. J Neurosci 15:214-222.

Zirpel L, Lippe WR, Rubel EW (1998) Activity-dependent regulation of [Ca2+]i in avian cochlear nucleus neurons: roles of protein kinases A and C and relation to cell death. J Neurophysiol 79:2288-2302.

Zirpel L, Janowiak MA, Veltri CA, Parks TN (2000a) AMPA receptor-mediated, calcium-dependent CREB phosphorylation in a subpopulation of auditory neurons surviving activity deprivation. J Neurosci 20:6267-6275.

Zirpel L, Janowiak MA, Taylor DA, Parks TN (2000b) Developmental changes in metabotropic glutamate receptor-mediated calcium homeostasis. J Comp Neurol 421:95-106.